# AtERF60 negatively regulates *ABR1* to modulate salt, drought, and basal resistance in Arabidopsis

**Running title: AtERF60 regulates stress response**

**Authors: Gajendra Singh Jeena[1#], Ujjal J Phukan[1#], Neeti Singh[1,2], Ashutosh Joshi[1], Alok Pandey[3], Yashraaj Sharma[1], Vineeta Tripathi[4], Rakesh Kumar Shukla[1,2]***

***Corresponding Author**

#- These authors contributed equally.

**Contact details,** 1. Plant Biotechnology Division, CSIR-Central Institute of Medicinal and Aromatic Plants, P.O. CIMAP, Lucknow-226015, India.

2. Academy of Scientific and Innovative Research (AcSIR), CSIR-Central Institute of Medicinal and Aromatic Plants (CSIR-CIMAP)

3. Microbial Technology Department, CSIR-Central Institute of Medicinal and Aromatic Plants, P.O. CIMAP, Lucknow-226015, India.

4. Ethanobotany Division, CSIR- Central Drug Research Institute, Jankipuram Extension, Sitapur Road, Lucknow-226031, India.

## ABSTRACT

ABSCISIC ACID REPRESSOR-1 (ABR1), an APETALA2 (AP2) domain containing transcription factor (TF) contribute important function against variety of external cues. Here, we report an AP2/ERF TF, AtERF60 that serves as an important regulator of *ABR1* gene. *AtERF60* is induced in response to drought, salt, abscisic acid (ABA), salicylic acid (SA), and bacterial pathogen *Pst*DC3000 infection. AtERF60 interacts with DEHYDRATION RESPONSE ELEMENTS (DRE1/2) and GCC box indicating its ability to regulate multiple responses. Overexpression of *AtERF60* results in the drought and salt stress tolerant phenotype in both seedling and mature Arabidopsis plants in comparison with the wild type (WT-Col). However, mutation in *AtERF60* showed hyperactive response against drought and salt stress in comparison with its overexpression and WT. Microarray and qRT-PCR analysis of overexpression and mutant lines indicated that AtERF60 regulates both abiotic and biotic stress inducible genes. One of the differentially expressing transcripts was *ABR1* and we found that AtERF60 interacts with the DRE *cis*-elements present in the *ABR1* promoter. The mutation in *AtERF60* showed ABA hypersensitive response, increased ABA content, and reduced susceptibility to *Pst*DC3000. Altogether, we conclude that *AtERF60* represses ABR1 transcript by binding with the DRE *cis*-elements and modulates both abiotic and biotic stress responses in Arabidopsis.

**Keywords**

Arabidopsis, AtERF60, ABR1, Abscisic acid, *Pst*DC3000, abiotic stress

## Introduction

Plants face multiple environmental stresses including various biotic and abiotic stresses which disturb their normal growth and development leading to massive agricultural losses (He et al., 2018). To adapt under these environmental conditions, plants have developed various evolutionary mechanisms governed through a complex regulatory network. TFs participate in regulating various interconnected and diverse signaling cascades by interacting with *cis*-elements present in their promoters (Liu et al., 2014). AP2/ERFs are one of the most important TF families that appeared as a key regulator of a large cluster of downstream target genes involved in various stress responses (Phukan et al., 2017). The AP2/ETHYLENE RESPONSIVE ELEMENT BINDING FACTOR (EREB) domain of AP2/ERFs is made up of conserved 40–70 amino acids that act as a DNA binding domain (Nakano et al., 2006). Based on the DNA binding domain, AP2/ERFs are classified into three groups, first is ERF (single ERF domain, contains subgroup I to X, VI-L and Xb-L), second is AP2 (tandem copies of two AP2 domains and few of them are with single AP2 domain) and third is RAV (ERF domain associated with a B3 DNA-binding domain). Soloist is a protein that contains an ERF domain, however its sequence and gene structure strongly diverge from ERF TFs (Shigyo and Ito, 2004, Nakano et al., 2006, Swaminathan et al., 2008, Zhuang et al., 2008; Licausi et al., 2010, Licausi et al., 2013). Together, these proteins are involved in integrating multiple phytohormone signals and regulate both abiotic and biotic stress responses (Gutterson and Reuber, 2004). ERF binds with the ETHYLENE-RESPONSE ELEMENT (ERE) or GCC-box to provide biotic stress resistance (Franco-Zorrilla et al., 2014).

Different properties of AP2/ERFs, including the DNA binding properties and induction upon various stresses, implement these TFs to coordinate multiple responses and participate in regulatory processes (Abiri et al., 2017). It is evident that AP2/ERFs and various phytohormones such as ethylene, Methyl jasmonate (MeJA), ABA, SA act in concert to regulate various plant processes (Licausi et al., 2013). The coordinated action of ABA and different abiotic stresses led to the activation of several stress-inducible genes and DREB2s (Lee et al., 2016). AP2/ERFs such as ABA-INSENSITIVE 4 (ABI4) and CBFA (CCAAT binding factor A) are ABA-responsive and help to activate the ABA-dependent/independent stress-responsive genes (Zhang et al., 2013). AP2/ERFs mutants with altered hormone sensitivity and abiotic stress responses have been identified and studied, mentioning this family of TFs as an important candidate to study the interactions between plant hormones and abiotic stresses.

The ERF subfamily protein is usually conscious to pathogen attack and contributes to plant immunity. Overexpression of ERF subfamily protein is usually related with altered disease resistance phenotypes in plants (Onate-Sanchez et al., 2007; Zhang et al., 2016; Zheng et al., 2019). Overexpression of rice *OsEREBP1* activates ABA and JA signaling pathways eventually resulted in enhanced tolerance under both biotic and abiotic conditions (Jisha et al., 2015). ABA regulates various important agronomical traits of plant development and physiology, such as seed dormancy and maturation, along with responses to several environmental stress factors, such as salinity, drought, and cold stress mediated through different components of ABA signaling (Himmelbach et al., 2003; Sah et al., 2016). During the investigation of gene expression regulated with ABA, an AP2-domain containing protein known as ABR1 was identified that acts as a negative regulator of ABA responses (Pandey et al., 2005). Later on, it was studied that ABR1 (group X of AP2/ERF) acts as a transcriptional activator and is involved in the wounding response (Baumler et al., 2019). ABR1 is an important molecule thought to play a functional role in the host-pathogen interface and acts as a susceptibility core that binds with different effector molecules of *Pseudomonas syringae* (Schreiber et al., 2021). Despite the importance of ABR1 involved in the regulation of both biotic and abiotic stress responses, its transcriptional regulator is not known. Here in our study, we have identified and characterized *AtERF60* (homologue of MaRAP2 from *Mentha arvensis*) (Phukan et al., 2018). We investigated that AtERF60 regulates *ABR1* gene by binding with their promoter and modulates both biotic and abiotic stress response in Arabidopsis.

## Results

### *AtERF60* is induced under salt, dehydration, ABA, and SA treatments

Sequencing analysis of *AtERF60* confirmed that the CDS of *AtERF60* is 819 bp in length, encoding a polypeptide of 273 amino acids. The alignment of complete ORF with its amino acid sequence has shown that it has a 58 amino acids conserved AP2/ERF DNA binding domain (DBD) (Fig. S1). Protein sequences of related AtERF60 among different plant species were recovered from Genbank to build the maximum likelihood phylogenetic tree. Phylogenetic homology of AtERF60 was studied utilizing MEGA6.06 software and found that it lies within the same clade and is closely related to the ERF of *Camelina sativa* and *Capsella rubella* (Fig. 1A). To investigate the evolutionary relation or diversity of AtERF60, we aligned the DBD of some closely related homologs from different plant species and found that the DBD of AtERF60 is closest to the AP2/ERF DBD of *Camelina sativa* (Fig. 1B). We studied the relative expression of *AtERF60* in response to salt, dehydration, wounding, ABA, SA, and methyl jasmonate (MeJA) treatments in *Arabidopsis thaliana* Col-0 plants. We observed that *AtERF60* is induced early after 1 hour of ABA treatment. *AtERF60* is maximally induced after 3 hours of salt and dehydration treatment, whereas the *AtERF60* showed a similar expression pattern

after 1 and 3 hours of SA treatment (Fig. 1C). Additionally, *AtERF60* is not induced in response to MeJA and wounding treatment as compared to the untreated control WT.

**AtERF60 interacts with DRE/GCC box *cis*-elements and can activate the reporter gene in yeast**

The recombinant GST-tagged-AtERF60 was induced and purified in bacterial expression system (Fig. S2A). An expected molecular mass of 56.0 kD along with GST-tagged-AtERF60 was observed and separated using SDS-PAGE (Fig. S2B). To study the DNA binding property of AtERF60, we performed EMSA of recombinant AtERF60 with DRE-1 and GCC-box *cis*-elements. Specific probes were designed for DRE-1 (GCCGAC) and GCC-box (AGCCGCC) *cis*-element along with their mutated forms containing a single nucleotide substitution (Fig. 2A). We found that AtERF60 interacts with DRE-1 and GCC-box *cis*-elements, while does not able to bind with its mutated probe carrying a change of single nucleotide (Fig. 2B). To study the transactivation property, we performed β-galactosidase activity in *Saccharomyces cerevisiae* (Y187 strain). We cloned *AtERF60* in pGBKT7 vector downstream of modified PT7 promoter fused with GAL4-DBD (Fig. 2C). *AtERF60* showed positive β-galactosidase activity utilizing ONPG as a substrate as compared to the vector control (Fig. 2D). We quantified the β-galactosidase activity and observed that AtERF60 has significantly higher β-galactosidase activity as compared to the vector control (Fig. 2E). The EMSA and β-galactosidase activity demonstrate that AtERF60 interacts with DRE-1 and GCC-box *cis*-elements and might be involved in the regulation of downstream target genes.

**AtERF60 provides resistance against salt and drought stress in Arabidopsis seedlings**

As it was observed that *AtERF60* was maximally induced under dehydration and salt stress treatments, and specifically interacts with DRE-1 and GCC-box *cis*-elements, therefore, we studied the regulatory role of AtERF60 under osmotic and dehydration stress in Arabidopsis. Overexpression lines (OX) under regulation of constitutive promoter CaMV35S and T-DNA insertion mutant (MT) lines of *AtERF60* were confirmed by semi-quantitative PCR using gene-specific primers (Fig. S3A). We also analyzed the expression level of *AtERF60* in these lines through qRT-PCR, which showed significantly increased *AtERF60* expression level (>4 folds) in the OX lines and reduced *AtERF60* expression level in MT lines (Fig. S3B). We provided drought and salt stress to *AtERF60*-OX and MT (*erf60*) lines to observe their stress response. Under control conditions, no phenotypic difference was observed in the *AtERF60*-OX and *erf60* mutant lines as compared to the WT seedlings. Under 200mM salt and 300mM mannitol stress conditions, WT seedlings exhibited reduced germination, growth, early senescence, and chlorosis, while *AtERF60*-OX and *erf60* mutant lines displayed resistant phenotype (Fig. 3A, B). However, an increased tolerance level was observed in the *erf60* mutant lines under salt and drought stress as compared to the *AtERF60*-OX lines. Total fresh weight

and chlorophyll content were observed to be significantly increased in both the *AtERF60*-OX and *erf60* mutant lines as compared to the WT seedlings. However, the *erf60* mutant plants showed better response, and higher total fresh weight and chlorophyll content as compared to the *AtERF60*-OX plants (Fig. 3C, D). This is particularly interesting because an increased tolerance level was observed in the *erf60* mutant lines under salt and drought stress as compared to the *AtERF60*-OX lines. These results suggest that AtERF60 is responsible for governing the abiotic stress tolerant phenotype in Arabidopsis plant.

**Loss of *AtERF60* function affects multiple gene expression**

To study the target genes influenced by AtERF60 in Arabidopsis, we performed a microarray analysis of both *AtERF60*-OX and *erf60* mutant lines under control conditions in two independent biological replicates (Table S1). We found that a total of 32 genes were downregulated (>2 folds) in the *AtERF60*-OX as compared to the *erf60* mutant with a significant P-value of <0.05 (Fig. 4A, Table S2). We further validated the expression of above identified genes using qRT-PCR analysis in both *AtERF60*-OX and MT lines as compared to the WT. We found that most of the genes encoding COMPROMIZED RECOGNITION OF TCV1 (CRT1), Peroxidase superfamily protein, Aspartyl protease family protein, O-glucosyl hydrolases family 17 protein, Alcohol dehydrogenase 1 (ADH1), Acyl-CoA synthetase 5 (ACS5), EIDI like 3, and ABR1 were significantly upregulated in the *erf60* mutant background as compared to the WT (Fig. 4B). Also, some of the genes encoding α/β hydrolases superfamily protein, Chalcone and Stilbene synthase family protein, MYB-like, Acyl-transferase family protein, and UDP-glycosyltransferase family protein were found to be upregulated in the *AtERF60*-OX as compared to the WT (Fig. 4B). The microarray and qRT-PCR analysis revealed that *AtERF60* might be involved in the regulation of these target genes directly or indirectly by binding with their promoter *cis*-elements. Therefore, we screened out the individual promoters and searched for the presence of probable *cis*-elements (Supplementary file 1).

**AtERF60 interacts with *ABR1* promoter**

Sequence analysis revealed the presence of dehydration (A/GCCGAC) and ABA-responsive *cis*-elements (ACGTC/G) in the *ABR1* promoter. Based on the presence of these core *cis*-elements in the *ABR1* promoter, we studied the interaction of AtERF60 with the *ABR1* promoter using EMSA. Probes specific to DRE and ABRE *cis*-elements were designed along with their mutated counterpart with a change in a single nucleotide (Fig. 5A). It was observed that AtERF60 interacts with both DRE-1 and DRE-2 *cis*-elements, while it does not able to produce gel shift with the ABRE *cis*-elements and its counterpart with a single nucleotide mutation (Fig. 5B). This showed that binding of AtERF60 is specific to A/GCCGAC *cis*-elements and is completely abolished when the sequence specific

nucleotide is mutated. To study the *in vivo* association of AtERF60 with *ABR1* promoter, we performed Y1H assay. The resulting *ABR1* promoter carrying the DRE1 and DRE2 *cis*-elements upstream of the *HIS3* reporter gene was cloned in the pHIS2.0 vector. After preparing the effector construct having *AtERF60* cloned in pGADT7, both the constructs were co-transformed in yeast *S. cerevisiae* (Y187 strain) under the selection media SD-*his*-*leu*. We found the positive Y1H interaction between the AtERF60 with the *ABR1* promoter as co-transformants were competent to grow in the selection media SD-*his*-*leu* media (Fig. 5C).

**Mutation in *AtERF60* resulted into hyperactive response against drought and salt stress**

To study the functional contribution of *AtERF60* in abiotic stress, we provided the salt and drought stress treatment to 5 weeks old Arabidopsis plants and regularly monitored the change in the phenotype on different days. The moisture content of soil was monitored at different days of drought stress, and the resulting phenotype was observed (Fig. S4 A-C). We found that *erf60* mutant plants are highly tolerant to drought and salt stress. However, overexpression of *AtERF60* resulted in reduced tolerance towards drought and salt stress as compared to the *erf60* mutant plants. Severe wilting, anthocyanin accumulation, chlorosis, and necrosis symptoms were observed in the WT and *AtERF60*-OX plants. It was also observed that *erf60* mutant plants sustained drought stress up to 12-14 days and salt stress up to 16-18 days (Fig. 6A, B). Plant samples were collected after six days of drought stress to study the relative expression of microarray validated genes using qRT-PCR analysis. We found that genes encoding CRT1, Aspartyl protease family protein, Chalcone and stilbene synthase family protein, ACS5, EIDI-like 3, and ABR1 were highly upregulated in the *erf60* mutant background as compared to the WT. Also, few genes encoding peroxidase superfamily protein, and CYP704B1 family protein were found to be upregulated in the *AtERF60*-OX as compared to the WT under drought stress (Fig. 6C). Based on the microarray data and qRT-PCR analysis under control and after drought stress, we observed that *ABR1, CRT1,* and *ACS5* are the common set of target genes that were highly induced in the *erf60* mutant plants as compared to the WT (Fig. 6C). Interestingly, *ABR1* was found to be down regulated in the *AtERF60*-OX and upregulated in the *erf60* mutant plants under drought stress conditions as compared to the WT. These results revealed that AtERF60 might be transcriptionally regulating the *ABR1* gene to modulate abiotic stress response in Arabidopsis.

***erf60* mutant showed hypersensitive response to ABA and delayed germination**

The specific interaction of AtERF60 with the *ABR1* promoter region prompts us to check the ABA sensitivity and germination rate of *AtERF60*-OX and *erf60* mutant seedlings. We observed that *erf60* mutants showed delayed seed germination as compared to WT. However, an opposite phenotype of early germination was observed in the *AtERF60*-OX lines as compared to WT seeds in the half MS

media (Fig. S5A). Also the percentage germination was found to be significantly reduced in the *erf60* mutants and increased in the *AtERF60*-OX lines as compared to WT seeds (Fig. S5B). To test the ABA hypersensitive response, we grew Arabidopsis seeds in the half MS media treated with the different concentrations of ABA. We observed that the mutant seeds exhibit a hypersensitive response to exogenous ABA at (6 µM) as compared to the WT and overexpression lines. The germination of *erf60* mutant seeds in half MS without ABA did not show any phenotypic difference as compared to the WT and OX lines (Fig. 7A). The germination percentage of seedlings were calculated after 2 weeks and compared to the WT seeds on the normal half MS medium. It was found that germination of *erf60* mutant seeds was significantly inhibited at 6 and 8 µM concentrations of ABA. The germination percentage of the *erf60* mutant seeds was significantly reduced to less than 30% at 6 µM and less than 20% at 8 µM ABA concentrations. We did not obtain much significant difference with an ABA concentration of less than 4 µM (Fig. 7B). Moreover, overexpression of *AtERF60* led to reduced sensitivity and a better germination rate (>70%) as compared to both WT and *erf60* mutants at the concentration of 6 and 8 µM ABA. These results suggest that mutation in the *AtERF60* renders the delayed germination and hypersensitive response to ABA in the Arabidopsis seedlings.

**AtERF60 regulates ABA content**

To study the regulatory role of AtERF60 in ABA biosynthesis, we determined the total ABA content in the *AtERF60*-OX and *erf60* mutant lines. Mature Arabidopsis plants of 18 days were utilized to determine the ABA content using HPLC. The peak obtained in the internal standard ABA was compared with the significant peak obtained in the plant samples at same retention time and relative quantification was performed. We observed that ABA content was significantly decreased in the *AtERF60*-OX lines and increased in the *erf60* mutant lines under control conditions as compared to WT (Fig. 7C). The ABA content in the *AtERF60*-OX lines was found to be 85.7 and 67.2 ng/g fresh wt respectively, which is significantly decreased as compared to WT (120.35 ng/g fresh wt). The ABA content in the *erf60* mutant lines (256.7 and 201.6 ng/g fresh wt) was observed to be significantly enhanced compared to WT and *AtERF60*-OX lines. This result suggests that AtERF60 negatively regulates the ABA content in the Arabidopsis.

**AtERF60 regulates defense response in Arabidopsis**

ABR1 is considered a functionally important molecule that interacts with different *Pseudomonas syringae* effectors (Schreiber et al., 2021). We sought to test our idea that AtERF60 regulates the central key component ABR1 and modulates plant response to biotic stress. To investigate the influence of *AtERF60* in biotic stress, we infiltrated Arabidopsis plants with *Pseudomonas syringae* pv. tomato (*Pst*) strain DC3000. The *AtERF60*-OX lines exhibited

increased chlorosis and necrosis at 4 days of post-inoculation (dpi), whereas *erf60* mutant lines displayed reduced disease symptoms as compared to the WT (Fig. 8A). Furthermore, the *erf60* mutant lines supported a significantly lower population of bacterial *Pst*DC3000 as compared to the WT. The bacterial population in the *erf60* mutant lines was reduced by 1.8 log ($CFU/cm^2$) representing a decrease of 71% after 4 dpi (Fig. 8B). A significant reduction in electrolyte leakage was observed in *erf60* mutant lines compared to the WT at 4 dpi with *Pst*DC3000 (Fig. 8C). In contrast to *erf60* mutant lines, significantly enhanced pathogen population and electrolyte leakage were observed in *AtERF60*-OX lines compared to the WT (Fig. 8B, C). Further, we used the confocal microscopy to follow the pathogen colonization in Arabidopsis plants using the GFP-tagged *Pst*DC3000 strain. *In vivo* imaging revealed the formation of the distinct microcolonies of GFP-tagged *Pst*DC3000 that were evenly dispersed in the intercellular spaces of leaves of WT (Fig. 8D). We observed reduced colonization of GFP-tagged *Pst*DC3000 in *erf60* mutant lines while *AtERF60*-OX lines displayed enhanced colonization of bacterial pathogen (Fig. 8D). Together, these results suggest that mutation in the *AtERF60* gene causes a reduction in susceptibility of Arabidopsis towards bacterial pathogen, *Pst*DC3000.

We examined the expression of *AtERF60* and *ABR1* genes in Arabidopsis plants following infection with *Pst*DC3000. The expression of the *AtERF60* and *ABR1* genes are strongly induced in WT in response to *Pst*DC3000 infection as observed at 6 hours post-inoculation (hpi) and 24 hpi. On the other hand, *ADH1, ACS, SOD,* and *CRT1* genes are not induced in response to the infection with *Pst*DC3000 (Fig. 8E). Also, the expression of *ABR1* is significantly induced and reduced in the *erf60* mutant and the *AtERF60*-OX plants, respectively, following the challenge with the *Pst*DC3000 (Fig. 8F, G). Thus, our data suggest a negative regulation of *ABR1* by AtERF60 under biotic stress.

## Discussion

AP2/ERFs are involved in regulating various downstream signaling cascades by interacting with different *cis*-elements of target gene promoters and regulate multiple responses (Phukan et al., 2018). In our study, we report that AtERF60 from Arabidopsis regulates abiotic and biotic stress tolerance by interacting and repressing the downstream target gene *ABR1*. In this study, we have identified a transcription factor, *AtERF60*, induced in response to drought conditions, salt stress, ABA/SA-treatment, and bacterial pathogen *Pst*DC3000 infection. Induction of the *AtERF60* in response to ABA and SA suggests that the *AtERF60* might be regulating abiotic and biotic stress responses in an ABA/SA-dependent manner. In Arabidopsis, *ERF53* (Hsieh et al., 2013), *RAP2.6* (Zhu et al., 2010), and *ERF-VIIs* (Yao et al., 2017) are induced in response to ABA to up-regulate the genes containing DRE/ABRE *cis*-elements. In addition, OsERF71 confers drought stress tolerance in rice by positively

regulating ABA signaling and root architecture (Li et al., 2018). There are limited number of AP2/ERFs reported to be involved in response to SA treatment (Xie et al., 2019). Interestingly, *AtERF60* was found to be induced in response to both ABA and SA treatment showing its possible involvement in young Arabidopsis seedlings both abiotic and biotic stress response through these two hormones or their cross-talk. The potential of AP2/ERFs to counter different signals and regulate multiple stresses facilitates them to make a highly complex stress regulatory network. Some AP2/ERFs are induced frequently, while others are induced upon prolonged stress, which suggests that their function might be influenced mutually (Van den Broeck et al., 2017).

The diversity of AP2/ERFs in response to various stresses depends on the flexibility of the AP2 domain that implements the binding to different *cis*-elements such as DRE/CRT and GCC-box elements (Huang et al., 2008, Cheng et al. 2013, Franco-Zorrilla et al., 2014, Catinot et al., 2015). Our previous study conclusively demonstrated that AP2/ERF TFs such as PsAP2 and MaRAP2-4 from the *Opium poppy* and *Mentha arvensis*, respectively, bind with both GCC and DRE box *cis*-elements to modulate biotic and abiotic stress response in transgenic plants (Mishra et al., 2015; Phukan et al., 2018). AtERF60 specifically interacts with both GCC and DRE box *cis*-elements, and is involved in the regulation of both biotic and abiotic stress response in Arabidopsis. We observed that it interacts with the core *cis*-element of DRE (GCCGAC), and the binding was abolished when we used the mutated version. We also observed that it interacts with the core GCC box element GCCGCC and mutation of the probe into GCCACC abolished its interaction. These results suggest that CCGCC is the core sequences which are preferred for AtERF60 to interact. If we mutate G of CCGCC to CCACC the binding was abolished. While for the DRE sequence we find that the mutation in last two CC to AC does not affect its affinity. Some ERFs including ERF71, ERF4, and ERF1 are also reported to interact with both DRE and ERE elements in Arabidopsis (Lee at al., 2015; Xie et al., 2019). The ability of AtERF60 to interact specifically with both DRE and GCC further supports its probable involvement in both abiotic and biotic stress response.

Additional insight into AtERF60 function in abiotic and biotic stress response was gained by processing and analyzing the microarray as well as expression data in both the overexpression and mutant background. Microarray analysis, promoter binding activity, and phenotypic studies suggest the regulatory role of AtERF60 in Arabidopsis. Here in our study, we found the interaction of AtERF60 with promoter of *ABR1*, but we have also reported the upregulation of target genes such as *CRT1*, Eukaryotic aspartyl protease family protein, Chalcone and Stilbene synthase gene, Acyl CoA synthase 5, EID1 like 3 protein in the *erf60* mutant plants after 6 days of drought stress. These are upregulated transcripts under stress condition in the *erf60* mutant plants might play a crucial role in regulating the abiotic ic stress tolerance in *erf60* mutant lines. Overexpression of *AtERF60* results in the upregulation of genes, such as alpha beta-hydrolyaze super family protein, MYB like HTH

protein, UDP glucosyltransferase superfamily protein, and these transcripts might be responsible for the improved salt and drought stress tolerance in *AtERF60* overexpression lines. The fold expressions of majority of differentially expressing transcripts are significantly high in the mutant background under control, drought and bacterial pathogen infection suggesting its better resistance against both abiotic and biotic stress. In addition to the ABA-mediated positive regulation of various AP2/ERFs in abiotic stress responses, several studies have shown that AP2/ERFs also hinder ABA signaling in Arabidopsis (Xie et al., 2019). Nonetheless, AP2/ERFs having an EAR motif or B3 repression domain showed a repressive effect on target genes (Kagale and Rozwadowski, 2011; Causier et al., 2012). AtERF7 negatively regulates stress response, overexpression of which showed reduced ABA sensitivity and increased water loss (Song et al., 2005). The better adaptability of *AtERF60* mutant plants than its overexpressing lines might be due to the increased ABA content in the mutant background and much higher expression of other stress related transcripts. The relationship of AtERF60 with other target genes which are differentially expressing in the mutant and overexpression background and its post-translational or transcriptional modification will further help us to understand its role in ABA or SA mediated signalling under abiotic/biotic stress response. Similarly, an AP2/ERF TF known as TINY was involved in regulating drought stress response in plants by modulating brassinosteroid mediated plant growth (Xie Z et al., 2019). AP2/ERF family TFs were also involved in improving drought tolerance by regulating the lignin biosynthesis and modifying the plant cell wall structure and growth (Lee et al., 2016). AP2/ERF is an important regulatory factor in the responsive pathway of salt stress signaling (Zhuang et al., 2008). Under salt stress conditions, a DREB subgroup TF known as SALT-RESPONSIVE ERF1 conducts signals through the MAP kinase cascade signaling pathway and inducing a salt stress response in plants (Schmidt et al., 2013).

*ABR1* gene is regulated by abiotic and biotic stress signals in plants. Mutation in *AtERF60*, an upstream regulator of the *ABR1* gene showed hypersensitive response to exogenous ABA. We believe that this response might be due to the increased ABA content in *erf60* mutant lines. To put it another way, altered stress sensitivity may be an ABA-dependent or ABA-independent phenomenon (Tuteja, 2007; Lim and Lee, 2020). AtERF60 regulates ABA signalling by targeting *ABR1* gene in an ABA dependent manner. ABR1 consists of a conserved RAYD element particularly involved in different protein-protein interactions and a conserved DNA binding YRG element typical of EREBPs (Okamuro et al., 1997). Computational predictions of ABR1 revealed various sequences like Short Linear Interaction Motifs (SLiMs) and Molecular Recognition Factors (MoRFs), which give platforms for binding several molecules (Vacic et al., 2007; Weatheritt and Gibson, 2012). ABR1 was first reported as a transcriptional repressor. However, later on, it was also observed that ABR1 has weak transcriptional activation activity due to the presence of the CACCG DNA-binding motif (Li et al., 2016).

In this study, mutation in *AtERF60* resulted in reduced susceptibility against bacterial pathogen *Pst*DC3000. In contrast, *AtERF60*-OX plants exhibited enhanced susceptibility to *Pst*DC3000. *AtERF60* and *ABR1* are induced in response to *Pst*DC3000 infection suggesting their involvement under biotic stress. This work identifies *AtERF60* as the pathogen-responsive gene for the first time. Similar to our observation, induction of Arabidopsis *ABR1* gene has been previously shown following infection with *Pst*DC3000 (Schreiber et al., 2021). ABR1 contributes to plant immunity by interacting with *Pseudomonas syringae* effector molecule HopZ1a along with other different effectors (Schreiber et al., 2021). Increased expression of *ABR1* in the *erf60* mutant plants in response to the pathogen infection suggests that AtERF60 influences the *ABR1* gene expression during biotic stress. Under the same condition, *ABR1* expression is repressed in *AtERF60*-OX plants. In this context, it is worth noting that *ABR1* overexpression transgenic lines of Arabidopsis exhibited enhanced resistance to biotrophic pathogens, *Pst* and *Hyaloperonospora arabidopsidis* (Choi and Hwang, 2011). Further, *ABR1* silencing in pepper plants led to the enhanced growth of *Xanthomonas campestris* pv. *vesicatoria* (Choi and Hwang, 2011). Our results suggest that AtERF60 plays an important role in the plant-pathogen interaction via negative regulation of *ABR1* expression. However, further studies would be required to get insights into AtERF60-mediated plant defense responses. Altogether, we conclude that AtERF60, an AP2/ERF TF negatively regulates *ABR1* gene in Arabidopsis under the control and abiotic/biotic stress conditions. The *erf60* mutant plants accumulate more ABA and exhibits enhanced resistance against drought and bacterial pathogen *Pst*DC3000.

## Materials and Methods

### Plant growth conditions and stress treatment

WT was grown according to the method followed by Phukan et al. (2017). WT seeds were surface sterilized (3% sodium hypochlorite solution), stratified at $4^0$C for 96 hours, and then transferred to the growth chamber under controlled conditions with photoperiod (16:8 h light-dark) at 22°C and 60% relative humidity. For salt stress in young Arabidopsis seedlings, WT seeds were grown in the plain half MS media for 7 days and then transferred to 200mM salt-containing half MS media. Salt stress treatment in 5- week old Arabidopsis plants in pots was provided by giving equal volume of 100mM NaCl solution at fixed time intervals. For drought stress treatment in young Arabidopsis seedlings, WT seeds were grown for two weeks in half MS media containing 300mM mannitol. Drought stress was provided to 5-week old Arabidopsis plants in pots by withholding water for 3-4 days. The moisture content of soil was measured with the soil moisture meter (Delmhorst, KS-D1). MeJA treatment was provided by spraying a 100 µM solution made in dimethyl sulfoxide (DMSO) and Triton-X. Control plants were sprayed with solution containing only DMSO and Triton- X. For SA and ABA treatment, plants were sprayed with 100 µM of SA and ABA, while control plants were

sprayed with water. The aerial part, including the stem and leaves, was punctured with a needle to avoid major injuries. To extract contaminations, treated samples were obtained at various periods and cleaned thoroughly with sterile water.

**Relative expression and phylogenetic analysis**

Total RNA was isolated from plant samples utilizing RNeasy (R) Plant Mini Kit (Qiagen), and cDNA was prepared utilizing high capacity cDNA reverse transcription kit (Applied biosystems). Total cDNA was checked for quality by performing PCR using the control primers provided in the kit. The qRT-PCR (Applied biosystems 7900-HT Fast Real-Time PCR) was performed to determine the expression level of transcripts utilizing SYBR Green PCR master mix kit (Takara). A unique region of transcripts was selected for designing qRT-PCR primers and mentioned in Table S3. Actin and ubiquitin were used as an endogenous control for normalizing gene expression. The $2^{-\Delta\Delta Ct}$ method was utilized to calculate the relative expression of genes.

The complete translated nucleotide sequence of *AtERF60* was deciphered by using the online Expasy translate tool (https://www.expasy.org/). Using AtERF60 as a query sequence, the BLASTp algorithm was used to find out the homologous protein sequences from various plant species. To examine the evolutionary relationship between various ERF60 homologs, MEGA 6.06 version was utilized to draw the phylogenetic tree using the maximum likelihood algorithm. The protein sequences that showed maximum homology with AtERF60 were selected to construct a phylogenetic tree and multiple sequence alignment analysis. The sequence alignment was performed by using clustal omega online program using default parameters (https://www.ebi.ac.uk/Tools/msa/clustalo/).

**Cloning experiments, generation of transgenic lines, and mutant screening**

The *AtERF60* was amplified by using gene-specific primers and cloned in PTZ57R/T vector. To analyze the *in vitro* interaction of protein and DNA, *AtERF60* was cloned in pGEX4T2 expression vector fused with GST. The positive clones were confirmed by PCR and digestion with primer-specific restriction enzymes (*Bam*HI and *Xho*I) (Fig. S6A). The resulting positive construct was transformed in Lon and OmpT protease deficient *E. coli BL21* (DE3) strain for expression in the bacterial system. To study the functional role of *AtERF60* in planta, we cloned it in pBI121 binary vector downstream of the CaMV35S promoter. The positive clones were confirmed by PCR and final digestion utilizing the specific restriction enzymes (*Bam*HI and *Xba*I) (Fig. S6B). The *AtERF60* transgenic lines in Arabidopsis were raised using the *Agrobacterium*-mediated gene transformation (Fig. S7A). Ten independent transgenic lines containing *AtERF60* were generated and two lines showing similar responses were used in the study. Transgenic lines in Arabidopsis were confirmed by using genomic DNA PCR using pBI-121 nptII ($Kan^R$) specific primers. The PCR amplification,

confirms the successful integration of desired gene (Fig. S7B). To determine the functional role of the *AtERF60*, we used T-DNA mutant lines of *AtERF60* (SALK_138492). The *erf60* mutants were screened by using genomic DNA PCR with specific primers designed from the left border of T-DNA (Fig. S8).

**Electrophoretic mobility shift assay and β-galactosidase activity**

To study the *in vitro* protein–DNA interaction, *AtERF60* was cloned in the bacterial expression vector pGEX4T2. The open reading frame was continued with GST without disturbing the amino acid sequences. The cloned construct was then transformed in Lon and OmpT protease deficient *E. coli BL21* (DE3) strain and induced with 0.4 mM IPTG at 37°C for 5 h. The recombinant fusion protein was purified with Glutathione Sepharose beads (Sigma). Definite probes were designed for different *cis*-elements as well as for their mutated versions (Table S3). EMSA was carried out by following the manufacture's protocol mentioned in the 2$^{nd}$ generation DIG gel shift kit (Roche). For performing the β-galactosidase activity, *AtERF60* was cloned in pGBKT7 and transformed in yeast Y187. The positive colonies in yeast were confirmed using colony PCR and grown overnight at 28°C. Cells were harvested and resuspended in Z-buffer. The β-galactosidase activity using ONPG as substrate was performed following the protocol mentioned in the yeast β-galactosidase assay kit (Thermo scientific).

**Yeast One-Hybrid (Y1H) assay**

Y1H assay was performed to study the *in vivo* protein DNA interaction. *AtERF60* was cloned in pGADT7 vector, and *ABR1* promoter fragment was cloned in pHIS-2.0 vector. Both the positive cloned constructs were co-transformed in yeast Y187 strain using lithium acetate (LiAc) mediated yeast transformation methods (Gietz and Schiest, 2007). The competent cells of yeast were prepared in a LiAc solution used for transformation. Positive cloned constructs along with the excess carrier DNA were transformed in the yeast competent cells. The positive colonies were screened by plating transformed yeast cells on selection media (SD-*His-Leu*). The positive colonies resulted in the selection media which confirms *in vivo* interaction were streaked in plain YPD and selection media (SD-*His-Leu*). All the yeast experiments were carried out following the yeast protocols handbook (Clontech).

**Total chlorophyll estimation**

Total chlorophyll was estimated from the leaf tissues as described previously in the protocol with minor modifications (Vernon, 1960). Total leaf tissue (approximately 100 mg) was taken and crushed into fine powder in liquid nitrogen and suspended in 80% chilled acetone. The extracted solution was centrifuged for 15-20 min 13000 rpm. The supernatant was then transferred to a fresh tube and the

pellet was discarded. Total volume was made up to 10 ml by adding 80% chilled acetone. The amount of total chlorophyll was calculated in mg/g fresh weight of the plant sample by taking absorbance at 663 nm and 645 nm as described in the protocol.

**Microarray analysis**

The complete RNA was extracted from the plant samples (WT, ERF60-OX, and *erf60* mutant) under controlled conditions utilizing the RNeasy (R) Plant Mini Kit (Qiagen) following the manufacturer's instructions. The Arabidopsis GXP 4x44K AMADID slide was used to hybridize the RNA, which was further aided and labeled with Cy3-CTP. The microarray was performed and scanned at 535 nm, and the images were analyzed using Agilent Feature Extraction software (v10.7) to calculate signal and background strength. The images obtained from the microarray were cleaned and are uniform in intensity, with very little background noise. For statistical significance and normalization, Gene-Spring GX 12.6 software was utilized. The values of fold induction obtained from two different lines were normalized to a single fold induction. The Student's t-test was used to correct P-values for downregulation and upregulation of genes in experimental and biological replicates. The P-value cut-off for gene up- and downregulation was set to <0.05.

**High performance liquid chromatography (HPLC)**

HPLC was performed to determine the ABA concentration in the WT, *AtERF60*-OX, and *erf60* mutant lines. The Arabidopsis plants were grown in half MS media and after 18 days plant samples were harvested and freeze dried in the liquid nitrogen. The ABA extraction protocol was followed as described in the methods with slight modifications (Forcat et al., 2008). Whole plant (10 mg fresh wt) was taken into the fresh centrifuge tubes and crushed in the 0.5 ml of 10% methanol containing 1% acetic acid. The supernatant was removed carefully and re-extracted in the same extraction buffer and incubated for 30 minutes in ice. The resulting extract (90-95% recovery) was utilized for the ABA quantification. Internal standard of ABA (Sigma) at different concentrations was utilized for making calibration plot (Fig. S9). The detection and quantification of ABA was performed in HPLC system (Waters 2696 with UV detector). Chromatographic separation was carried out on a C18 column (4.6×250 mm, 5 µm) maintained at 25°C with a gradient elution having the flow rate of 0.6 ml/min. Solvent A (Acetonitrile) and Solvent B (0.1% phosphoric acid solution) was used as mobile phase. The gradient elution program was set up accordingly: 20% A and 80% B (0 min), 25% A and 75% B (5 min), 30% A and 70% B (8 min), 35% A and 65% B (15 min), 45% A and 55% B (25 min). The ABA was quantified by using the calibration plot based on the peak areas at the maximum wavelength of 260 nm.

### Bacterial pathogen assays with *Pseudomonas syringae* pv. tomato DC3000 (*Pst*DC3000)

Bacterial pathogen *Pst*DC3000 was grown at 28°C overnight on LB media containing 50µg/ml rifampicin. For infiltration, bacteria were re-suspended in 10 mM $MgCl_2$ to obtain $OD_{600}$ = 0.2. The leaves of 5-week-old WT, *AtERF60*-OX, and *erf60* Arabidopsis plants were syringe infiltrated with *Pst*DC3000. Disease symptoms were observed at regular intervals and photographed. Bacterial populations [Log (CFU/$cm^2$)] in leaf tissues of WT, *AtERF60*-OX, and *erf60* plants at 0, 2, and 4 dpi, were determined according to Katagiri et al. (2002). For electrolyte leakage assay, 4 leaf discs of the equal-area (0.5 $cm^2$) were taken from each WT, *AtERF60*-OX, and *erf60* plants inoculated with *Pst*DC3000 at 4 dpi. These leaf discs were then agitated in a tube containing 10 ml milli-Q water for 3 h. The conductivity was measured using the electrical conductivity meter for each sample (HORIBA Scientific, F74BW). Afterward, leaf discs for each sample were autoclaved to release the total ions, and conductivity corresponding to total ions was measured. Electrolyte leakage values (conductivity value at 3 h) were presented as the percentage relative to total ions.

Pathogen colonization in Arabidopsis plants was visualized using Zeiss confocal laser-scanning microscope (LSM-880). We used GFP-tagged *Pst*DC3000 for this assay. Confocal images of leaf samples of WT, *AtERF60*-OX, and *erf60* plants inoculated with GFP-tagged *Pst*DC3000 were taken at 2 dpi. GFP acquisition was performed at 488 nm excitation with emission collection at 493-598 nm. For leaf red chlorophyll autofluorescence, excitation at 633 nm and emission collection at 647-721 was used. Image processing was performed using Zeiss application software. Leaf samples from Arabidopsis plants were collected at 6 and 24 hpi to examine the expression of selected genes in response to *Pst*DC3000 challenge using the qRT-PCR assay. For the control, leaves were infiltrated with 10 mM $MgCl_2$. Actin and ubiquitin were used as endogenous control for gene normalization.

### Statistical analysis

The experiments in the study were performed in two independent biological replicates each with three technical repeats. The data shown in the study are mean $\pm$ SD. Student t-test was performed using instat.exe version 3.0 software to measure the degree of significance with P-value $\leq 0.05$ is significant and denoted by an asterisk above the bar graph in the figures. A double asterisk denotes a higher level of significance with a P-value $\leq 0.01$.

### Acknowledgements

Authors acknowledge Director, CSIR-CIMAP for providing necessary facilities. Authors acknowledge ABRC for providing the mutant seeds of AtERF60. We also acknowledge Genotypic for performing the microarray analysis of overexpression and mutant background of AtERF60.

## Funding

RKS acknowledge CSIR-CIMAP and SERB for financial support to his lab. GSJ, UJP, AJ, NS acknowledge CSIR-UGC for fellowship and YS acknowledge CSIR-network project for fellowship. AP is grateful to DST - INSPIRE Faculty Award (IFA13-LSPA-20).

## Author contributions

GSJ has performed the affinity purification and gel retardation, reporter gene activation, q-RT PCR validation, performed the abiotic stress response in seedlings, transgenic analysis of bigger plants and abiotic stress response, ABA sensitivity, and ABA content measurement, biotic stress response of *erf60* mutant and overexpression lines. UJP has made the cloning constructs of AtERF60, made overexpression lines, and screened the *erf60* mutant lines, provided samples for microarray analysis. GSJ, and YS has performed ABA sensitivity experiment. NS has performed Arabidopsis seed germination analysis of overexpression and mutant lines. She has also helped in performing the abiotic stress and biotic stress response of overexpression and mutant lines. AJ and NS have performed soil moisture content analysis for drought stress experiment. AJ has helped in performing ABA analysis and total chlorophyll estimation in Arabidopsis plants. AP created GFP-tagged *Pst*DC3000 strain and supervised the bacterial pathogen assays in the Arabidopsis plants and confocal microscopy study and edited the text. VT has contributed in planning of experiment related to mutant background and procuring of mutant background of AtERF60, GSJ has made the first draft of manuscript, RKS has supervised the work, analyzed the result, planned the experiments and edited the manuscript. GSJ, AP, AJ and RKS have finalized the draft manuscript.

## Data Availability Statement

ERF60- AT4G39780, ADH 1- AT1G77120, ACOS5- AT1G62940, Chalcone and stilbene synthase- AT4G34850, CYP450 family protein- AT1G69500, Aspartyl protease family protein- AT5G24820, Actin 1- AT2G37620, Acyl-transferase family protein- AT1G03390, EID1-like 3- AT3G63060, ABR1- AT5G64750, CRT1- AT4G36290, alpha/beta-Hydrolases superfamily protein- AT1G73480, O-Glycosyl hydrolases family 17 protein- AT4G14080, Myb-like HTH transcriptional regulator family protein- AT1G18960, UDP-Glycosyltransferase superfamily protein- AT1G10400, RING/U-box superfamily protein- AT1G49220, Microarray data deposited with the accession number GSE179600.

## Conflict of interest

The authors declare no conflict of interest.

## References

**Abiri R, Shaharuddin NA, Maziah M, Yusof ZNB, Atabaki N, Sahebi M, et al.** (2017) Role of ethylene and the APETALA 2/ethylene response factor superfamily in rice under various abiotic and biotic stress conditions. Environ. Exp. Bot **134**: 33–44.

**Bartlett A, O'Malley RC, Huang SC, Galli M, Nery JR, Gallavotti A, et al.** (2017) Mapping genome-wide transcription-factor binding sites using DAP-seq. Nat. Protoc **12**: 1659–1672.

**Baumler J, Riber W, Klecker M, Müller L, Dissmeyer N, Weig AR, et al.** (2019) AtERF111/ABR1 is a transcriptional activator involved in the wounding response. Plant J **100(5)**: 969-990.

**Catinot J, Huang JB, Huang PY, Tseng MY, Chen YL, Gu SY, et al.** (2015) ETHYLENE RESPONSE FACTOR 96 positively regulates Arabidopsis resistance to necrotrophic pathogens by direct binding to GCC elements of jasmonate and ethylene responsive defence genes. Plant, cell & environment **38(12)**: 2721–2734.

**Causier B, Ashworth M, Guo W, Davies B** (2012) The TOPLESS interactome: a framework for gene repression in Arabidopsis. Plant Physiol **158**: 423–438.

**Cheng MC, Liao PM, Kuo WW, Lin TP** (2013) The Arabidopsis ETHYLENE RESPONSE FACTOR1 regulates abiotic stress-responsive gene expression by binding to different cis-acting elements in response to different stress signals. Plant Physiology **162**: 1566–1582.

**Choi DS, Hwang BK** (2011) Proteomics and functional analyses of pepper abscisic acid-responsive 1 (ABR1), which is involved in cell death and defense signaling. Plant Cell **23**: 823-42.

**Forcat S, Bennett MH, Mansfield JW, Grant MRA** (2008) rapid and robust method for simultaneously measuring changes in the phytohormones ABA, JA and SA in plants following biotic and abiotic stress. Plant methods **4**, 16.

**Franco-Zorrilla JM, Lopez-Vidriero I, Carrasco JL, Godoy M, Vera P, Solano R** (2014) DNA-binding specificities of plant transcription factors and their potential to define target genes. Proc. Natl. Acad. Sci. U.S.A. **111**: 2367–2372.

**Gietz RD, Schiest RH** (2007) High-efficiency yeast transformation using the LiAc/SS carrier DNA/PEG method. Nat Protoc **2(1)**: 31-34.

**Gutterson N, Reuber TL** (2004) Regulation of disease resistance pathways by AP2/ERF-transcription factors. Curr. Opin. Plant Biol **7**: 465–471.

**He M, He CQ, Ding NZ** (2018) Abiotic Stresses: General Defenses of Land Plants and Chances for Engineering Multistress Tolerance. Frontiers in plant science **9**: 1771.

**Himmelbach A, Yang Y, Grill E** (2003) Relay and control of abscisic acid signaling. Curr Opin Plant Biol **6**: 470–479.

564 **Huang D, Wu W, Abrams SR, Cutler AJ** (2008) The relationship of drought-related gene
565 expression in Arabidopsis thaliana to hormonal and environmental factors. J. Exp. Bot **59**: 2991–
566 3007.
567 **Hsieh EJ, Cheng MC, Lin TP** (2013) Functional characterization of an abiotic stress-inducible
568 transcription factor AtERF53 in Arabidopsis thaliana. Plant Mol. Biol **82**: 223–237.
569 **Jisha V, Dampanaboina L, Vadassery J, Mithofer A, Kappara S, Ramanan R** (2015)
570 Overexpression of an AP2/ERF Type transcription factor OsEREBP1 confers biotic and abiotic stress
571 tolerance in rice. PLoS ONE **10**: e0127831.
572 **Kagale S, Rozwadowski K** (2011) EAR motif-mediated transcriptional repression in plants: an
573 underlying mechanism for epigenetic regulation of gene expression. Epigenetics **6**: 141–146.
574 **Katagari F, Thlimony R, He SY** (2002) The Arabidopsis *thaliana- Pseudomonas*
575 *syringae* interaction. Arabidopsis Book **1**: e0039
576 **Lee DK, Jung H, Jang G, Jeong JS, Kim YS, Ha SH, et al.** (2016) Overexpression of the OsERF71
577 transcription factor alters rice root structure and drought resistance. Plant Physiol **172(1)**: 575–588.
578 **Lee SY, Boon NJ, Webb AA, Tanaka RJ** (2016) Synergistic Activation of RD29A via integration of
579 salinity stress and abscisic acid in Arabidopsis thaliana. Plant Cell Physiol **57**: 2147–2160.
580 **Lee SY, Hwang EY, Seok HY, Tarte VN, Jeong MS, Jang SB, et al.** (2015) Arabidopsis
581 AtERF71/HRE2 functions as transcriptional activator via cis-acting GCC box or DRE/CRT element
582 and is involved in root development through regulation of root cell expansion. Plant Cell Rep **34**:
583 223–231.
584 **Li J, Guo X, Zhang M, Wang X, Zhao Y, Yin Z, et al.** (2018) OsERF71 confers drought tolerance
585 via modulating ABA signaling and proline biosynthesis. Plant Science **270**, 131–139.
586 **Li T, Wu XY, Li H, Song JH, Liu JY** (2016) A dual-function transcription factor, AtYY1, is a novel
587 negative regulator of the Arabidopsis ABA response network. Mol. Plant **9**: 650–661.
588 **Licausi F, Giorgi F, Zenoni S, Osti F, Pezzotti M, Perata P** (2010) Genomic and transcriptomic
589 analysis of the AP2/ERF superfamily in Vitis vinifera. BMC Genomics **11**: 719.
590 **Licausi F, Ohme-Takagi M, Perata P** (2013) APETALA2/Ethylene Responsive Factor (AP2/ERF)
591 transcription factors: mediators of stress responses and developmental programs. New Phytol **199**:
592 639–649.
593 **Lim CW, Lee SC** (2020) ABA-Dependent and ABA-Independent Functions of RCAR5/PYL11 in
594 Response to Cold Stress. Frontiers in plant science **11**: 587620.
595 **Liu JH, Peng T Dai W** (2014) Critical cis-Acting Elements and Interacting Transcription Factors:
596 Key Players Associated with Abiotic Stress Responses in Plants. Plant Mol Biol Rep **32**: 303–317.
597 **Mishra S, Phukan UJ, Tripathi V, Singh DK, Luqman S, Shukla RK** (2015) PsAP2 an AP2/ERF
598 family transcription factor from papaver somniferum enhances abiotic and biotic stress tolerance in
599 transgenic tobacco. Plant Mol. Biol **89**: 173–186.

Nakano T, Suzuki K, Fujimura T, Shinshi H (2006) Genome-wide analysis of the ERF gene family in Arabidopsis and rice. Plant Physiol **140:** 411–432.

**Okamuro JK, Caster B, Villarroel R, Montagu M, Van and Jofuku KD** (1997) The AP2 domain of APETALA2 defines a large new family of DNA binding proteins in Arabidopsis. Proc. Natl. Acad. Sci. U.S.A. **94**: 7076–7081.

**Oñate-Sánchez L, Anderson JP, Young J, Singh KB** (2007) AtERF14, a member of the ERF family of transcription factors, plays a nonredundant role in plant defense. Plant physiology **143(1)**: 400–409.

**Pandey GK, Grant JJ, Cheong YH, Kim BG, Li L, Luan S** (2005) ABR1, an APETALA2-domain transcription factor that functions as a repressor of ABA response in Arabidopsis. Plant Physiol **139(3)**: 1185-93.

**Phukan UJ, Jeena GS, Tripathi V, Shukla RK** (2018) MaRAP2-4, a waterlogging responsive ERF from Mentha, regulates bidirectional sugar transporter AtSWEET10 to modulate stress response in Arabidopsis. Plant Biotechnol J **16(1)**: 221-233.

**Phukan UJ, Jeena GS, Triptahi V, Shukla RK** (2017) Regulation of Apetala2/Ethylene Response Factors in Plants. Frontiers in Plant Science **8**: 150.

**Sah SK, Reddy KR, Li J** (2016) Abscisic Acid and Abiotic Stress Tolerance in Crop Plants. Frontiers in plant science **7**: 571.

**Sakuma Y, Liu Q, Dubouzet JG, Abe H, Shinozaki K, Yamaguchi-Shinozaki K** (2002) DNA-binding specificity of the ERF/AP2 domain of Arabidopsis DREBs, transcription factors involved in dehydration- and cold-inducible gene expression. Biochem. Biophys. Res. Commun **290**: 998–1009.

**Schmidt R, Mieulet D, Hubberten HM, et al.** (2013) Salt-responsive ERF1 regulates reactive oxygen species-dependent signaling during the initial response to salt stress in rice. Plant Cell **25(6)**: 2115–2131.

**Schreiber KJ, Hassan JA, Lewis JD** (2021) Arabidopsis Abscisic Acid Repressor 1 is a susceptibility hub that interacts with multiple Pseudomonas syringae effectors. The Plant journal: for cell and molecular biology **105(5)**: 1274–1292.

**Shigyo M, Ito M** (2004) Analysis of gymnosperm two-AP2-domain-containinggenes. Development Genes and Evolution **214**: 105–114.

**Song CP, Agarwal M, Ohta M, Guo Y, Halfter U, Wang P, et al.** (2005). Role of an Arabidopsis AP2/EREBP-type transcriptional repressor in abscisic acid and drought stress responses. Plant Cell **17**: 2384–2396.

**Swaminathan K, Peterson K, Jack T** (2008) The plant B3 superfamily. Trends inPlant Science **13**: 647–655.

**Tuteja N** (2007) Abscisic Acid and abiotic stress signaling. Plant Signal Behav **2(3)**: 135-138.

635 **Vacic V, Oldfield CJ, Mohan A, Radivojac P, Cortese MS, Uversky VN Dunker AK** (2007)
636 Characterization of molecular recognition features, MoRFs, and their binding partners. J. Proteome
637 Res **6**: 2351–2366.
638 **Van den Broeck L, Dubois M, Vermeersch M, Storme V, Matsui M, Inze D** (2017) From network
639 to phenotype: the dynamic wiring of an Arabidopsis transcriptional network induced by osmotic
640 stress. Mol. Syst. Biol **13**: 961.
641 **Vernon LP** (1960) Spectrophotometric determination of chlorophylls and pheophytins in plant
642 extracts. Anal. Chem **23**: 1144–1150.
643 **Weatheritt RJ, Gibson TJ** (2012) Linear motifs: lost in (pre) translation. Trends Biochem. Sci **37**:
644 333–341.
645 **Xie Z, Nolan T, Jiang H, et al.** (2019) The AP2/ERF Transcription factor TINY modulates
646 brassinosteroid regulated plant growth and drought responses in Arabidopsis. Plant Cell **31(8)**:1788–
647 1806.
648 **Xie Z, Nolan TM, Jiang H, Yin Y** (2019) AP2/ERF Transcription Factor Regulatory Networks in
649 Hormone and Abiotic Stress Responses in Arabidopsis. Frontiers in plant science **10**: 228.
650 **Yao Y, Chen X, Wu AM** (2017) ERF-VII members exhibit synergistic and separate roles in
651 Arabidopsis. Plant Signal. Behav **12**: e1329073.
652 **Zhang H, Hong Y, Huang L, Li D, Song F** (2016) Arabidopsis AtERF014 acts as a dual regulator
653 that differentially modulates immunity against Pseudomonas syringae pv. tomato and Botrytis cinerea.
654 Sci. Rep **6**: 1–15.
655 **Zhang ZW, Feng LY, Cheng J, Tang H, Xu F, Zhu F, et al.** (2013) The roles of two transcription
656 factors, ABI4 and CBFA, in ABA and plastid signalling and stress responses. Plant Mol. Biol **83**:
657 445–458.
658 **Zheng X, Xing J, Zhang K, Pang X, Zhao Y, Wang G, et al.** (2019) Ethylene response factor
659 ERF11 activates BT4 transcription to regulate immunity to Pseudomonas syringae. Plant Physiol **180**:
660 1132–1151.
661 **Zhu Q, Zhang J, Gao X, Tong J, Xiao L, Li W, et al.** (2010) The Arabidopsis AP2/ERF
662 transcription factor RAP2.6 participates in ABA, salt and osmotic stress responses. Gene **457**: 1–12.
663 **Zhuang J, Cai B, Peng RH, Zhu B, Jin XF, Xue Y, et al.** (2008) Genome-wide analysis of the
664 AP2/ERF gene family in Populus trichocarpa. Biochem Biophys Res Commun **371(3)**: 468–474.
665

666 **Figure legends**

667 **Figure 1.** Phylogenetic analysis and expression study of AtERF60. **(A)** Maximum likelihood
668 phylogenetic tree was constructed using MEGA6.06 showed that AtERF60 is closely related to the
669 ERF of *Camelina sativa* and *Capsella rubella* and lies within the same clade. The numbers represent

the bootstrap values. Only bootstrap values greater than 50% are shown. The scale represents the number of substitutions per site. **(B)** Clustal Omega alignment of AtERF60 protein showed their conserved DNA binding domain is highly similar to *Camelina sativa*. Protein sequences were retrieved from NCBI database and selected based on the maximum homology with AtERF60 protein. **(c)** Relative expression of *AtERF60* transcript in response to salt, dehydration, SA, wounding, ABA and MeJA treatment after 1, 3, and 5 h. Relative expression of transcripts was calculated taking untreated plant samples as a control (WT). Actin and ubiquitin were used as an endogenous control for gene normalization. Error bars indicate mean ± SD. Student's t-test, **, $P < 0.01$.

**Figure 2.** EMSA and β-galactosidase activity of recombinant AtERF60 protein purified from *Escherichia coli* (BL21 strain). **(A)** Probes containing DRE (GCCGAC) and GCC-box (AGCCGCC) *cis*-elements were designed to study the DNA-protein interaction. The desired *cis*-elements are marked with red color while the binding site carrying mutations are highlighted with blue colour. **(B)** EMSA of AtERF60 showed that it specifically interacts with DRE-1 and GCC regulatory *cis*-elements (M-mutated/substituted and L-DIG-labelled). **(C)** Representation of cloned *AtERF60* in pGBKT7 vector downstream of PT7 vector fused with GAL4-DBD. **(D)** The β-galactosidase activity of AtERF60 in yeast *S. cerevisiae* (Y187 strain). AtERF60 showed positive β-galactosidase activity (develops yellow color using ONPG as a substrate) as compared to the vector control. I and II represents the two different sets of experiments performed in triplicates. **(E)** β-galactosidase units (Miller units) were determined as follows: $1{,}000 \times OD420/ (t \times V \times OD660)$, where t is the incubation time and V is volume of culture. Error bars indicate mean ± SD. Student's t-test, **, $P < 0.01$.

**Figure 3.** *erf60* mutants showed better tolerance to salt and drought stress in Arabidopsis seedlings. **(A)** Growth of *AtERF60*-OX lines in MS media containing salt and mannitol as compared to the WT. The WT seedlings showed reduced growth, chlorosis, and senescence as compared to the *AtERF60*-OX lines under salt and drought stress. **(B)** Growth of *erf60* mutant lines in MS media containing salt and mannitol as compared to the WT. The *erf60* mutant lines showed better growth response as compared to the WT seedlings. No sign of chlorosis and senescence was observed in mutant plants. Seeds were grown on MS media for one week before being moved to media supplemented with 200 mM NaCl for one week. Seeds were geminated on MS media containing 300 mM mannitol for 2 weeks to induce dehydration stress. **(C)** Total fresh weight (mg) and **(D)** Chlorophyll content (mg/g fresh weight, line-1) in the *AtERF60*-OX and MT lines after 2 weeks of salt and dehydration treatment as compared to the WT seedlings. Error bars indicate mean ± SD. Student's t-test, *, $P < 0.05$; **, $P < 0.01$.

**Figure 4.** Microarray analysis and *in vitro* validation of selected target genes in the *AtERF60*-OX and *erf60* mutant plants under controlled conditions. **(A)** Heat map showing the induced expression of

target genes obtained after microarray analysis. Most of the target genes were found to be upregulated in the *erf60* mutant plants as compared to the *AtERF60*-OX plants. Color scale represents the $\log_2$ fold change values. **(B)** Relative expression of target genes as determined by qRT-PCR in the *AtERF60*-OX and *erf60* mutant lines as compared to the WT. The expression of target genes in the *erf60* mutant background corroborates with the microarray data. Actin and ubiquitin were used as an endogenous control for gene normalization. Error bars indicate mean ± SD. Student's t-test, *, $P < 0.05$; **, $P < 0.01$.

**Figure 5.** AtERF60 interacts with both DRE1 and DRE2 *cis*-elements present in the *ABR1* promoter. **(A)** Probes containing DRE1/2 (A/GCCGAC) and ABRE1/2 (ACGTC/G) *cis*-elements were designed to study the DNA-protein interaction. The desired *cis*-elements are marked with red colour while the binding site containing mutations are marked with blue colour. **(B)** EMSA of AtERF60 showed that it specifically interacts with the regulatory DRE1 and DRE2 *cis*-elements present in the *ABR1* promoter whereas it does not interact with the ABRE1/2 *cis*-elements (M-mutated/substituted and L-DIG-labelled). **(C)** Yeast one-hybrid (Y1H) assay was performed in yeast Y187 strain to study the *in vivo* interaction of AtERF60 with *ABR1* promoter carrying the probable *cis*-elements. The effector (AtERF60-pGAD) and reporter (ABR1 promoter-pHIS2.0) constructs were generated and co-transformed in yeast Y187. The positive colonies containing the resulting co-transformants obtained in the selection media (SD-*his*-*leu*) were streaked and shown.

**Figure 6.** *erf60* mutant plants showed enhanced drought and salt tolerance phenotype in mature Arabidopsis plants. **(A)** Phenotype of *AtERF60*-OX and *erf60* mutant plants as compared to the WT after different days of severe drought stress. Drought stress is provided to 5-week old Arabidopsis plants in pots after withholding water for 3-4 days. **(B)** Phenotype of *AtERF60*-OX and *erf60* mutant plants as compared to the WT after different days of salt stress. The salt stress was induced by giving equal amount of 100mM NaCl solution at fixed time intervals. The *erf60* mutant plants showed enhanced drought and salt stress tolerant phenotype as compared to the WT. **(C)** Relative expression of target genes was determined by qRT-PCR after 6 days of drought stress in the *AtERF60*-OX and *erf60* mutant lines as compared to the WT. Actin and ubiquitin were used as an endogenous control for gene normalization. Error bars indicate mean ± SD. Student's t-test, *, $P < 0.05$; **, $P < 0.01$.

**Figure 7.** *erf60* mutants showed enhanced sensitivity to exogenous ABA in Arabidopsis seedlings. **(A)** The hypersensitivity to exogenous ABA was observed in the *erf60* mutants at 6µM concentration, whereas *AtERF60*-OX plants showed insensitivity towards ABA treatment. **(B)** Percentage germination rate in the *AtERF60*-OX and *erf60* mutant plants after different ABA concentrations (µM) as compared to the WT. **(C)** ABA content (ng/g fresh weight) in the WT, *AtERF60*-OX and

*erf60* mutant lines after 18 days of seed germination under control conditions. Error bars indicate mean ± SD. Student's t-test, **, P < 0.01.

**Figure 8.** *erf60* mutants exhibit reduced susceptibility to *Pst*DC3000. **(A)** Disease symptoms in leaves of WT, *AtERF60*-OX and *erf60* mutant lines inoculated with *Pst* DC3000. Photographs were taken in triplicates at 4 days post-inoculation (dpi). **(B)** Bacterial growth in leaves of WT, *AtERF60*-OX and *erf60* mutant lines inoculated with *Pst*DC3000 at 0, 2, and 4 dpi. **(C)** Electrolyte leakage from leaves of WT, *AtERF60*-OX and *erf60* mutant lines inoculated with *Pst*DC3000 at 4 dpi. Electrolyte leakage values are given as the percentage of total ions. **(D)** Confocal images of leaves of WT, *AtERF60*-OX and *erf60* mutant lines with GFP-tagged *Pst*DC3000 at 2 dpi. For GFP acquisition, 488 nm excitation and 493-598 nm emission were used, whereas, for leaf red chlorophyll autofluorescence, 633 nm excitation, and 647-721 emission were used. GFP fluorescence (green), chlorophyll autofluorescence (red), and merge of both signals are shown. Scale bar represents 100 µm. **(E)** Expression analysis of *ABR1, ERF60, ADH1, ACS, SOD,* and *CRT1* genes in WT following infection with *Pst* DC3000 at 6 hours post-inoculation (hpi) and 24 hpi are presented relative to WT infiltrated with 10mM $MgCl_2$. *ABR1* and *ERF60* are induced in response to pathogen *Pst*DC3000. **(F)** Relative expression of *ABR1, ADH1, ACS, SOD,* and *CRT1* genes in the *AtERF60*-OX and *erf60* mutants following infection with *Pst*DC3000 relative to the WT infected with *Pst* DC3000 at 6 hpi and 24 hpi. **(G)** Relative expression of *ABR1* gene in the *AtERF60*-OX and *erf60* mutants infected with *Pst*DC3000 at 24 hpi relative to *AtERF60*-OX and *erf60* plants infiltrated with 10mM $MgCl_2$. Actin and ubiquitin were used as an endogenous control for gene normalization. Error bars indicate mean ± SD. Student's t-test, *, P < 0.05; **, P < 0.01.

## Supplementary data

**Figure S1.** Nucleotide and amino acid alignment of AtERF60. Complete cDNA (1224 bp) carrying 819 bp of ORF. Red colour represents amino acid sequence and blue colour represent AP2/ERF DNA binding domain. *AtERF60* has a 145 bp 5' UTR and 259 bp of 3' UTR. It encodes a protein of 273 amino acids having a molecular weight of 30kD.

**Figure S2.** Protein induction and purification of AtERF60. **(A)** 56 kD GST fused AtERF60 protein was induced with different concentration (mM) of IPTG at $37^0$C. **(B)** Recombinant AtERF60 protein was purified from *E. coli* BL21 (DE3) strain. The recombinant protein was induced for 5 hours at $37^0$C with 0.3 mM IPTG and affinity purified with sepharose GST beads. An affinity purified recombinant protein with a molecular weight of 56.0 kD and GST-tagged recombinant protein was segregated on SDS-PAGE.

**Figure S3. (A)** Semi-quantitative PCR to confirm the overexpression and mutation of *AtERF60* in two different lines along with WT. Actin was used as an internal control. **(B)** Relative expression of *AtERF60* in the OX and MT plants as compared to the WT using qRT-PCR analysis. The data was normalized relative to actin as an endogenous control. Error bars indicate mean ± SD. Student's t-test, **, $P < 0.01$.

**Figure S4. (A)** Total moisture content of dry and water saturated soil at two different days of drought stress. **(B)** Total moisture content of soil containing Arabidopsis plants at two different days of drought stress. **(C)** Phenotype of Arabidopsis plants after 1 and 20 days of drought stress. The *erf60* mutant lines showed enhanced tolerance to drought stress as compared to the WT plants.

**Figure S5. (A)** Delayed germination in the *erf60* mutants observed after one week of seed plating in the half MS media. **(B)** Percentage germination of the ERF60-OX and mutant lines as compared with the WT. Error bars indicate mean ± SD. Student's t-test, **, $P < 0.01$.

**Figure S6.** Cloning and generation of transgenic lines of *AtERF60*. **(A)** Confirmation of positive clones of *AtERF60* by PCR and digestion in bacterial expression vector pGEX4T2. **(B)** Confirmation of positive clones of *AtERF60* in pBI121 vector by PCR and digestion.

**Figure S7. (A)** Selection of transgenic lines on kanamycin supplemented half MS media. **(B)** PCR confirmation of transgenic lines. Genomic DNA PCR of transgenic lines with NPT II (KanR) primers.

**Figure S8.** Mutant screening of *AtERF60*. Genomic DNA PCR of mutant *AtERF60* Salk lines. LB- left border, RP- right primer, LP- left primer. The resulting amplification using primers specific LB and RP showed mutant homozygous lines.

**Figure S9.** Calibration plot of internal standard ABA (Sigma) at different concentrations (ng/ml). The linearity graph was plotted based upon the resulting peak areas at different concentrations.

**Supplementary file 1.** List of selected Arabidopsis promoter sequences used in the study.

**Table S1.** Microarray data showing list of up and downregulated genes obtained.

**Table S2.** List of genes identified from microarray analysis with significant p-value (<0.05).

**Table S3.** List of primers used in the study.

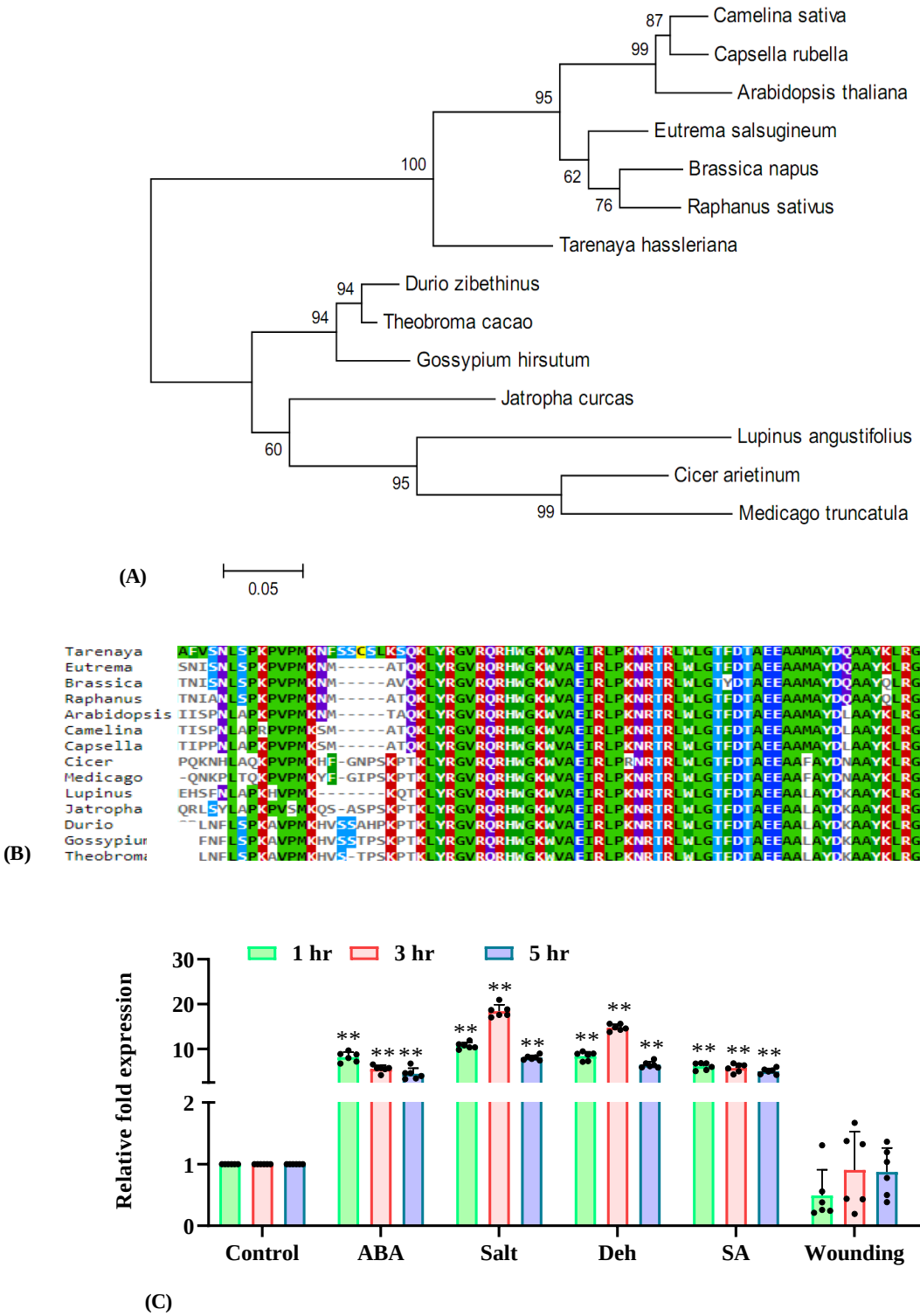


**Figure 1.** Phylogenetic analysis and expression study of AtERF60. **(A)** Maximum likelihood phylogenetic tree was constructed using MEGA6.06 showed that AtERF60 is closely related to the ERF of *Camelina sativa* and *Capsella rubella* and lies within the same clade. The numbers represent the bootstrap values. Only bootstrap values greater than 50% are shown. The scale represents the number of substitutions per site. **(B)** Clustal Omega alignment of AtERF60 protein showed their conserved DNA binding domain is highly similar to *Camelina sativa*. Protein sequences were retrieved from NCBI database and selected based on the maximum homology with AtERF60 protein. **(C)** Relative expression of *AtERF60* transcript in response to 1, 3, and 5 hours of salt, dehydration, SA, wounding, ABA and MeJA treatment. Relative expression of transcripts was calculated taking untreated plant samples as a control (WT). Actin and ubiquitin were used as an endogenous control for gene normalization. Error bars indicate mean ± SD. Student's t-test, **, $P < 0.01$.

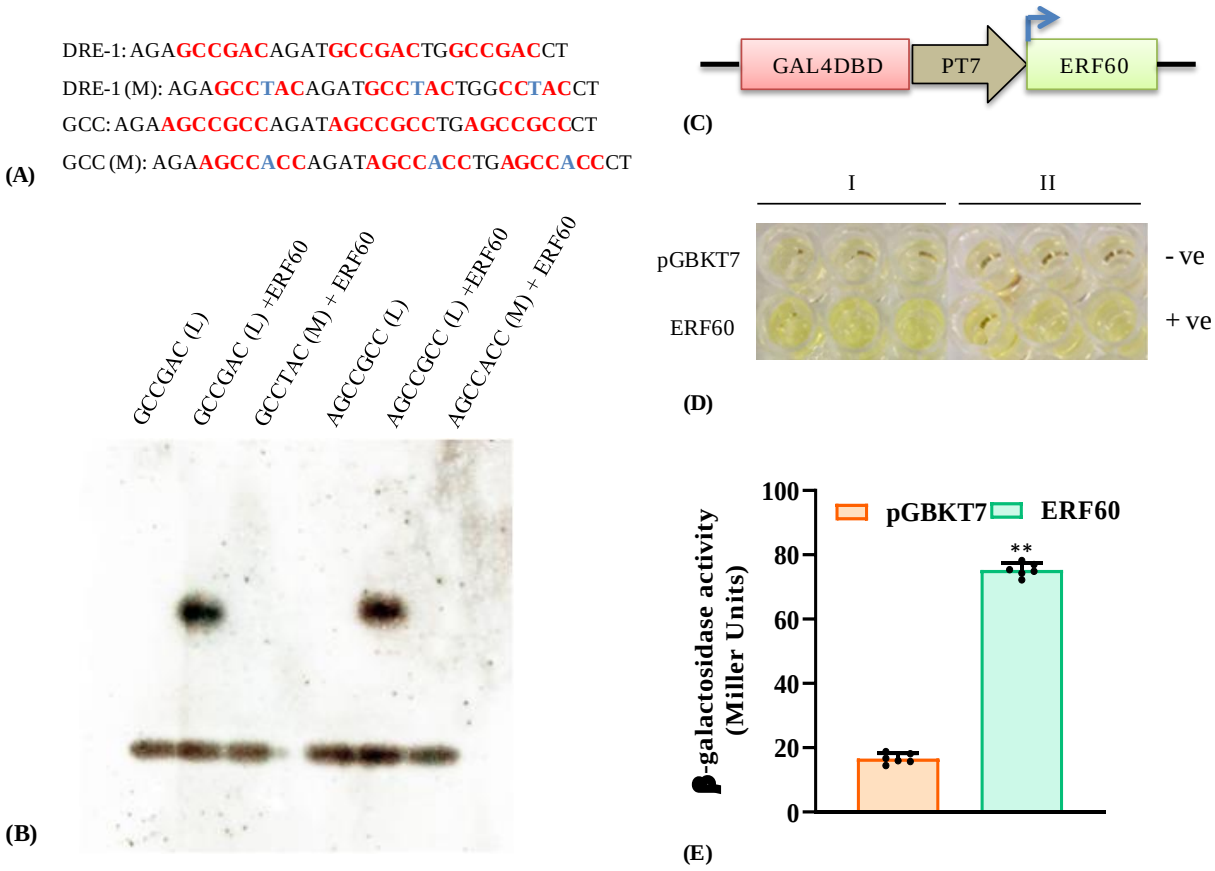


**Figure 2.** EMSA and β-galactosidase activity of recombinant AtERF60 protein purified from *Escherichia coli* (BL21 strain).**(A)** Probes containing DRE (GCCGAC) and GCC-box (AGCCGCC) *cis*-elements were designed to study the DNA-protein interaction. The desired *cis*-elements are marked with red color while the binding site carrying mutations are highlighted with blue color. **(B)** EMSA of AtERF60 showed that it specifically interacts with DRE-1 and GCC regulatory *cis*-elements (M-mutated/substituted and L-DIG-labelled). **(C)** Representation of cloned *AtERF60* in pGBKT7 vector downstream of PT7 vector fused with GAL4-DBD. **(D)** The β-galactosidase activity of AtERF60 in yeast *S. cerevisiae* (Y187 strain). AtERF60 showed positive β-galactosidase activity (develops yellow color using ONPG as a substrate) as compared to the vector control. I and II represents the two different sets of experiments performed in triplicates. **(E)** β-galactosidase units (Miller units) were determined as follows: 1,000 × OD420/ (t × V × OD660), where t is the incubation time and V is volume of culture. Error bars indicate mean ± SD. Student's t-test, **, $P < 0.01$.

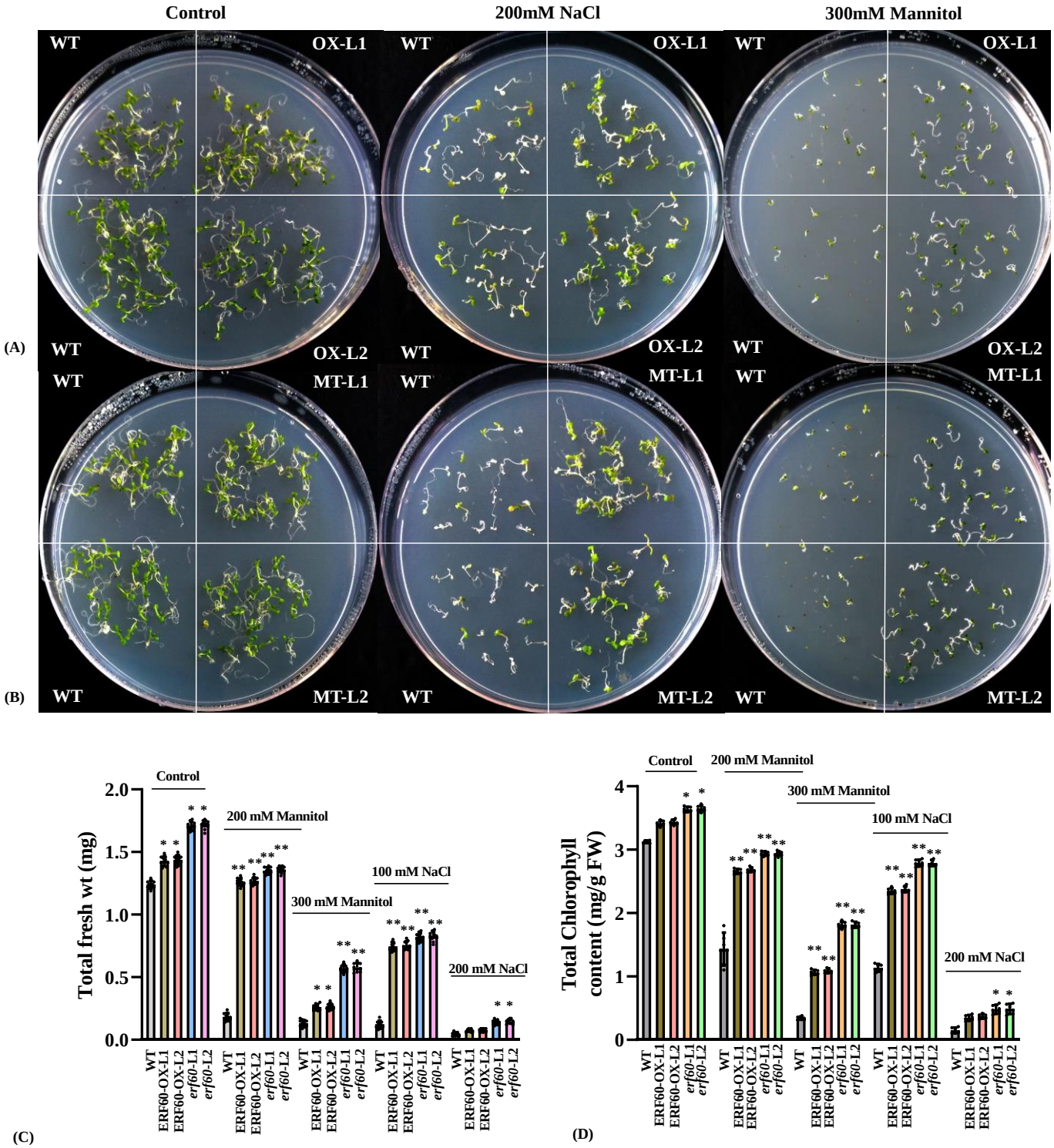


**Figure 3.** *erf60* mutants showed better tolerance to salt and drought stress in *Arabidopsis* seedlings. **(A)** Growth of *AtERF60*-OX lines in MS medium containing salt and mannitol as compared to the WT. The WT seedlings showed reduced growth, chlorosis, and senescence as compared to the *AtERF60*-OX lines under salt and drought stress. **(B)** Growth of *erf60* mutant lines in MS media containing salt and mannitol as compared to the WT. The *erf60* mutant lines showed better growth response as compared to the WT seedlings. No sign of chlorosis and senescence was observed in mutant plants. Seeds were grown on MS media for one week before being moved to media supplemented with 200mM NaCl for one week. Seeds were geminated on MS media containing 300mM mannitol for 2 weeks to induce dehydration stress. **(C)** Total fresh weight (mg) and **(D)** Chlorophyll content (mg/g fresh weight, line-1) in the *AtERF60*-OX and MT lines after 2 weeks of salt and dehydration treatment as compared to the WT seedlings. Error bars indicate mean ± SD. Student's t-test, *, $P < 0.05$; **, $P < 0.01$.

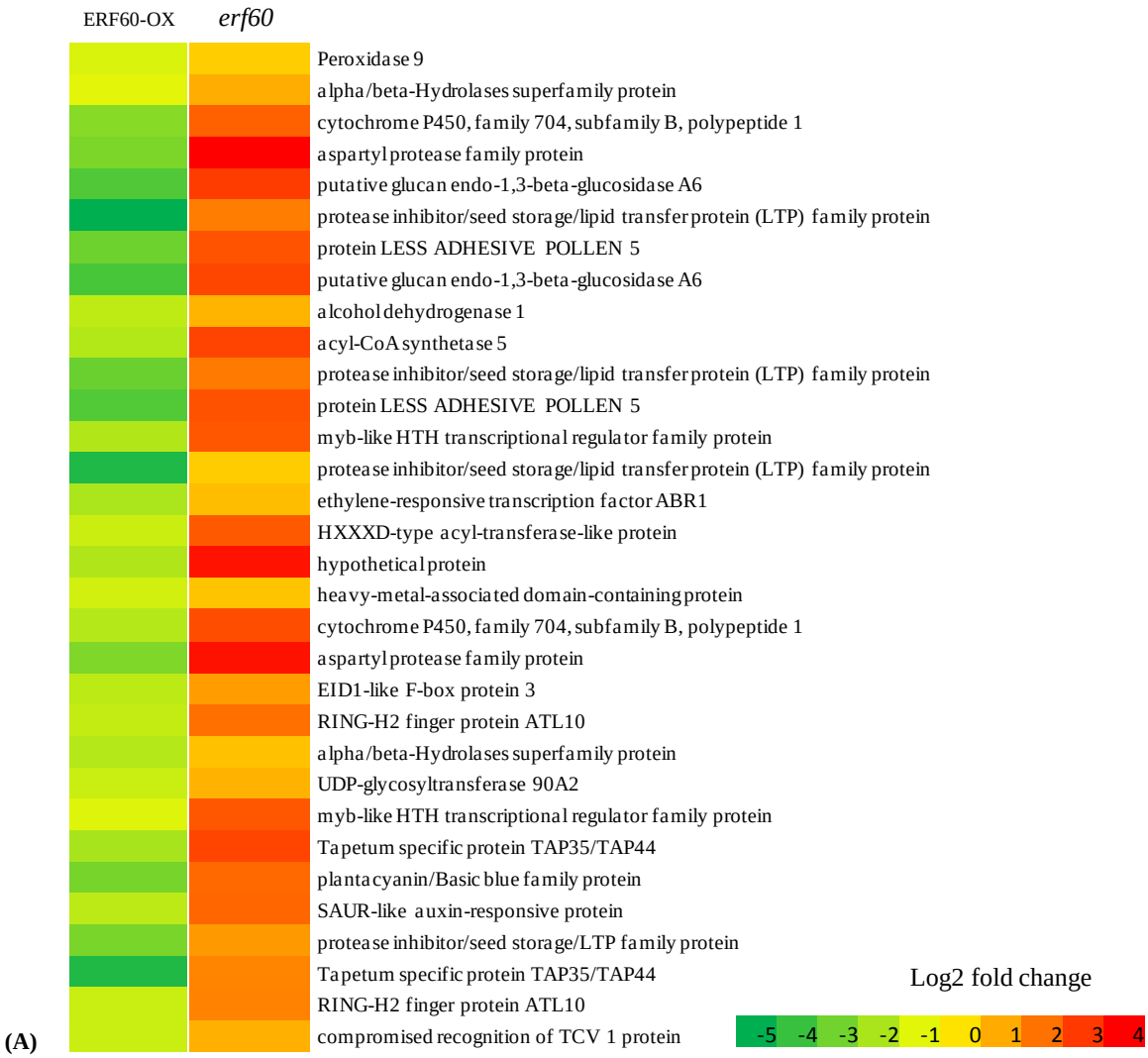


**Figure 4.** Microarray analysis and *in vitro* validation of selected target genes in the *AtERF60*-OX and *erf60* mutant plants under controlled conditions. **(A)** Heat map showing the induced expression of target genes obtained after microarray analysis. Most of the target genes were found to be upregulated in the *erf60* mutant plants by 2-4 folds as compared to the *AtERF60*-OX plants. Color scale represents the $\log_2$ fold change values. **(B)** Relative expression of target genes as determined by qRT-PCR in the *AtERF60*-OX and mutant lines as compared to the WT. The expression of target genes in the *erf60* mutant background corroborates with the microarray data. Actin and ubiquitin were used as an endogenous control for gene normalization. Error bars indicate mean ± SD. Student's t-test, *, $P < 0.05$; **, $P < 0.01$.

**(A)**

DRE-1: AGAGCCGACAGATGCCGACTGGCCGACCT
DRE-1 (M): AGAGCCTACAGATGCCTACTGGCCTACCT
DRE-2: AGAACCGACAGATACCGACTGGCCGCCCT
DRE-2 (M): AGAACCTACAGATACCTACTGACCTACCT
ABRE-1: AGAACGTCAGATACGTCTGACGTCCT
ABRE-1 (M): AGAACATCAGATACATCTGACATCCT
ABRE-2: AGAACGTGAGATACGTGTGACGTGCT
ABRE-2 (M): AGAACATCAGATACATCTGACATCCT

**(B)**

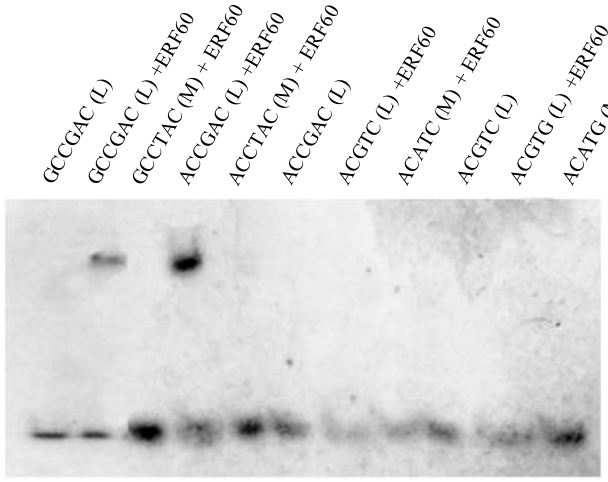


**(C)**

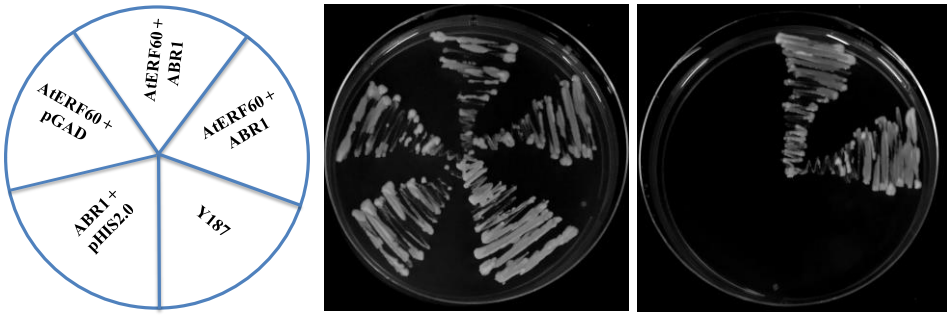


**Figure 5.** AtERF60 interacts with both DRE1 and DRE2 *cis*-elements present in the *ABR1* promoter. **(A)** Probes containing DRE1/2 (A/GCCGAC) and ABRE1/2 (ACGTC/G) *cis*-elements were designed to study the DNA-protein interaction. The desired *cis*-elements are marked with red color while the binding site containing mutations are marked with blue color. **(B)** EMSA of AtERF60 showed that it specifically interacts with the regulatory DRE1 and DRE2 *cis*-elements present in the *ABR1* promoter whereas it does not interact with the ABRE1/2 *cis*-elements (M-mutated/substituted and L-DIG-labelled). **(C)** Yeast one-hybrid (Y1H) assay was performed in yeast Y187 strain to study the *in vivo* interaction of AtERF60 with *ABR1* promoter carrying the probable *cis*-elements. The effector (AtERF60-pGAD) and reporter (ABR1 promoter-pHIS2.0) constructs were generated and co-transformed in yeast Y187. The positive colonies containing the resulting co-transformants obtained in the selection media (SD-*his*-*leu*) were streaked and shown.

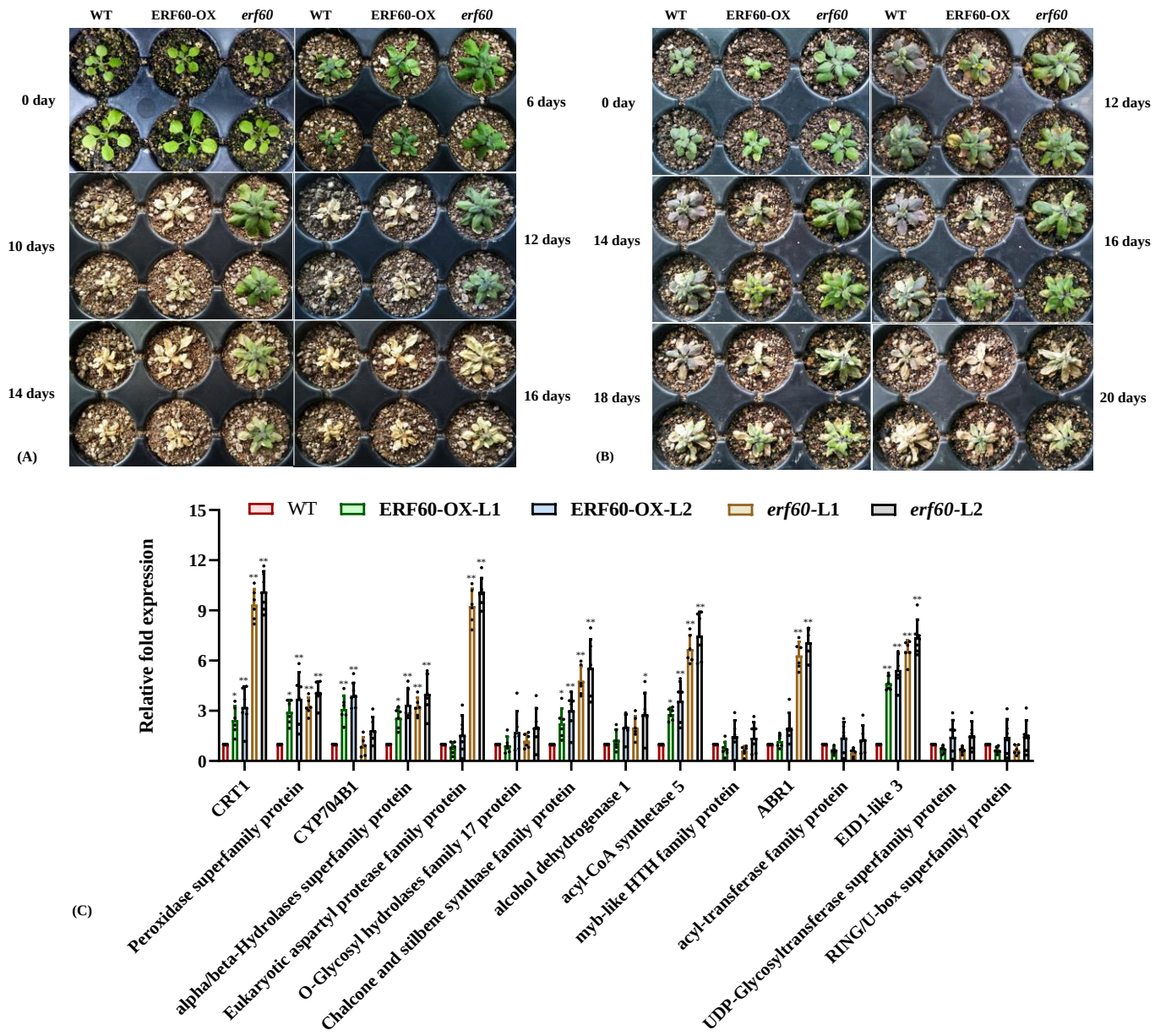


**Figure 6.** *erf60* mutant plants showed enhanced drought and salt tolerance phenotype in mature *Arabidopsis* plants. **(A)** Phenotype of *AtERF60*-OX and mutant (MT) plants as compared to the WT after different days of severe drought stress. Drought stress is provided to 5 week old *Arabidopsis* plants in pots after withholding water for 3-4 days. **(B)** Phenotype of *AtERF60*-OX and MT plants as compared to the WT after different days of salt stress. The salt stress was induced by giving equal amount of 100mM NaCl solution after fixed time intervals. The *erf60* mutant plants showed enhanced drought and salt stress tolerant phenotype as compared to the WT. **(C)** Relative expression of target genes was determined by qRT-PCR after 6 days of drought stress in the *AtERF60*-OX and MT lines as compared to the WT. Actin and ubiquitin were used as an endogenous control for gene normalization. Error bars indicate mean ± SD. Student's t-test, *, $P < 0.05$; **, $P < 0.01$.

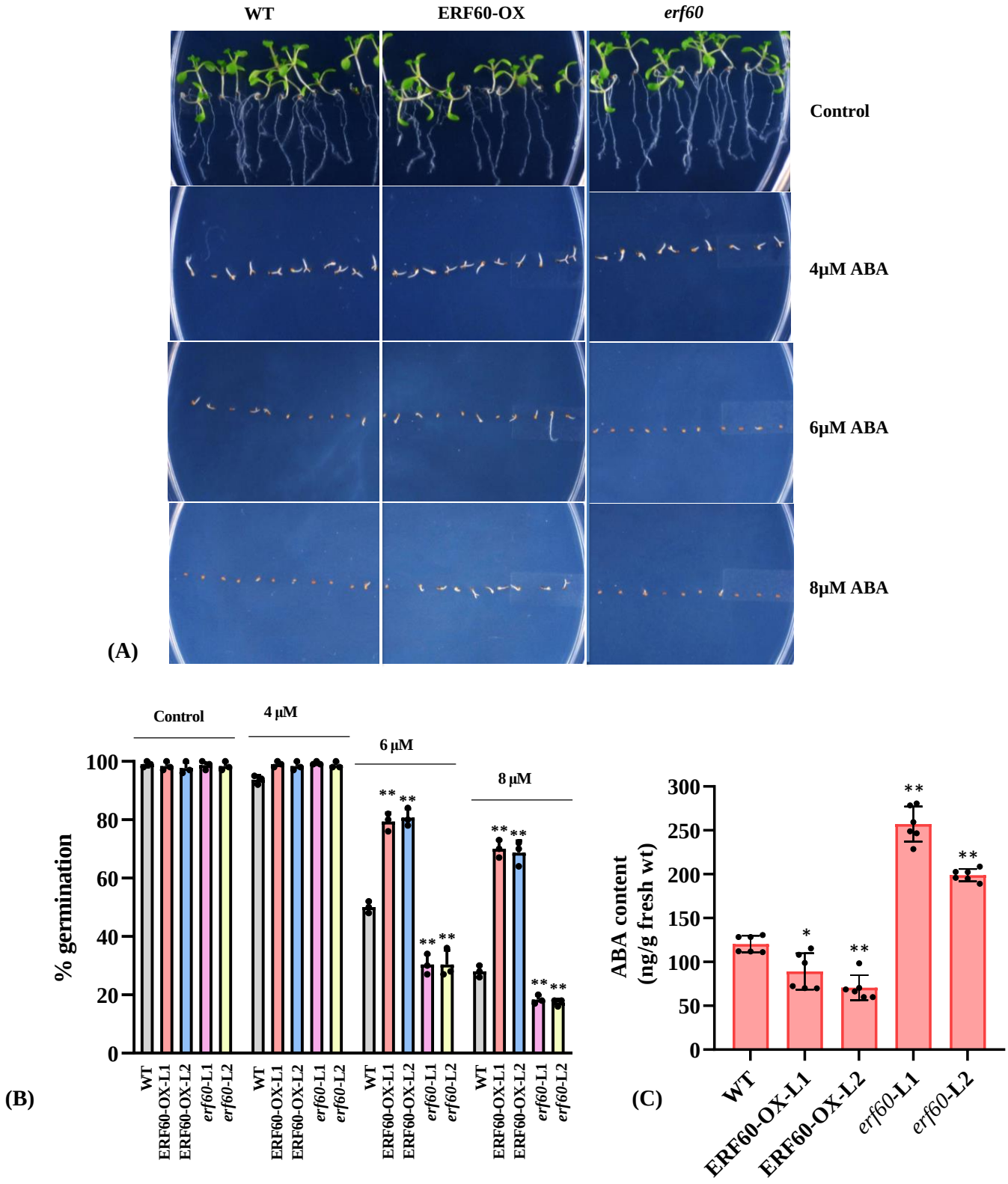


**Figure 7.** *erf60* mutants showed enhanced sensitivity to exogenous ABA in *Arabidopsis* seedlings. **(A)** The hypersensitivity to exogenous ABA was observed in the *erf60* mutants at 6µM concentration, whereas *AtERF60*-OX plants showed insensitivity towards ABA treatment. **(B)** Percentage germination rate in the *AtERF60*-OX and *erf60* mutant plants after different ABA concentrations (µM) as compared to the WT. **(C)** ABA content (ng/g fresh weight) in the WT, *AtERF60*-OX and *erf60* mutant lines after 18 days of seed germination under control conditions. Error bars indicate mean ± SD. Student's t-test, **, $P < 0.01$.

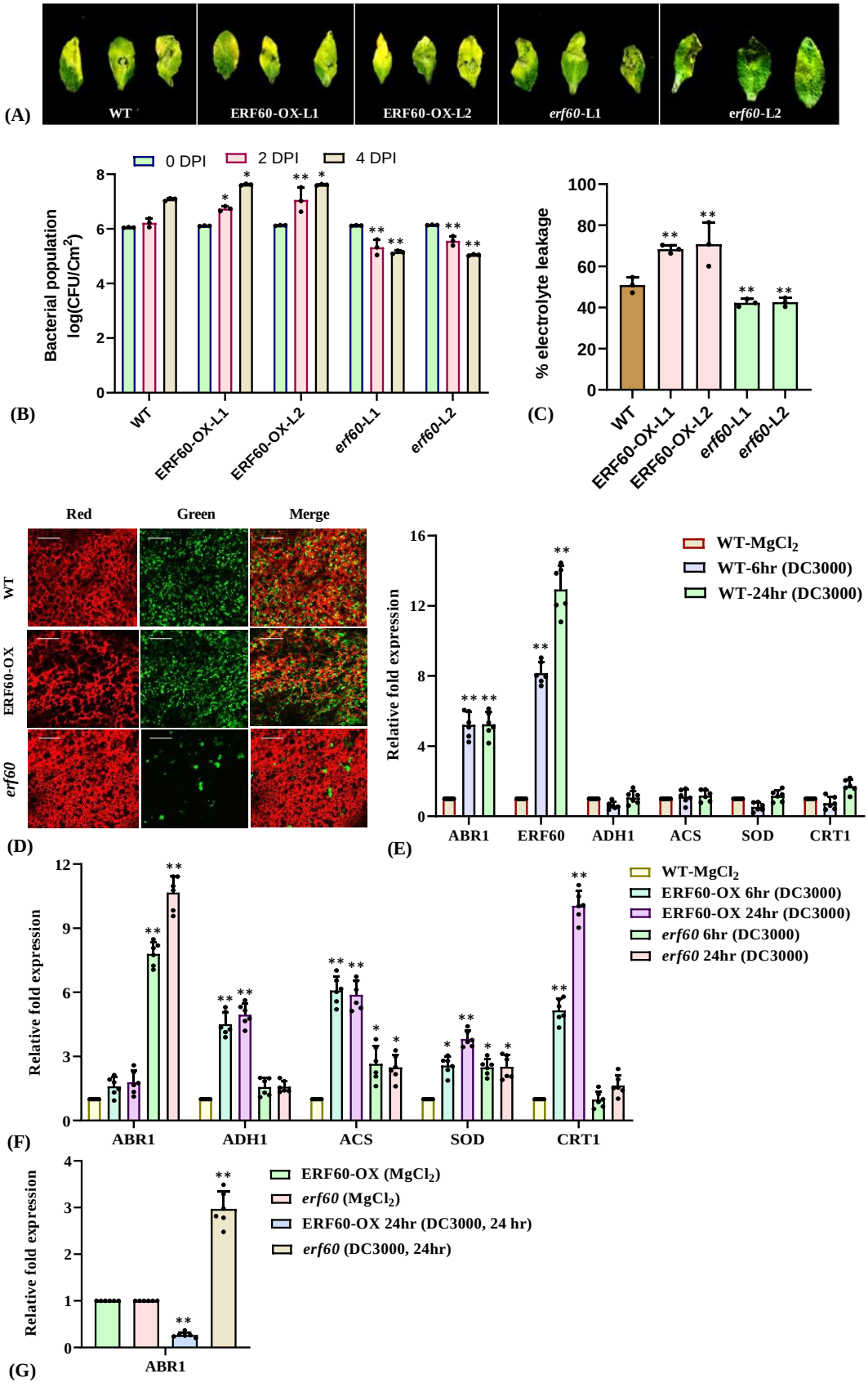


**Figure 8.** *erf60* mutants exhibit reduced susceptibility to *Pst*DC3000. **(A)** Disease symptoms in leaves of WT, *AtERF60*-OX and *erf60* mutant lines inoculated with *Pst* DC3000. Photographs were taken in triplicates at 4 days post-inoculation (dpi). **(B)** Bacterial growth in leaves of WT, *AtERF60*-OX and *erf60* mutant lines inoculated with *Pst*DC3000 at 0, 2, and 4 dpi. **(C)** Electrolyte leakage from leaves of WT, *AtERF60*-OX and *erf60* mutant lines inoculated with *Pst*DC3000 at 4 dpi. Electrolyte leakage values are given as the percentage of total ions. **(D)** Confocal images of leaves of WT, *AtERF60*-OX and *erf60* mutant lines with GFP-tagged *Pst*DC3000 at 2 dpi. For GFP acquisition, 488 nm excitation and 493-598 nm emission were used, whereas, for leaf red chlorophyll autofluorescence, 633 nm excitation, and 647-721 emission were used. GFP fluorescence (green), chlorophyll autofluorescence (red), and merge of both signals are shown. Scale bar represents 100 µm. **(E)** Expression analysis of *ABR1, ERF60, ADH1, ACS, SOD,* and *CRT1* genes in WT following infection with *Pst* DC3000 at 6 hours post-inoculation (hpi) and 24 hpi are presented relative to WT infiltrated with 10mM $MgCl_2$. *ABR1* and *ERF60* are induced in response to pathogen *Pst*DC3000. **(F)** Relative expression of *ABR1, ADH1, ACS, SOD,* and *CRT1* genes in the *AtERF60*-OX and *erf60* mutants following infection with *Pst*DC3000 relative to the WT infected with *Pst* DC3000 at 6 hpi and 24 hpi. **(G)** Relative expression of *ABR1* gene in the *AtERF60*-OX and *erf60* mutants infected with *Pst*DC3000 at 24 hpi relative to *AtERF60*-OX and *erf60* plants infiltrated with 10mM $MgCl_2$. Actin and ubiquitin were used as an endogenous control for gene normalization. Error bars indicate mean ± SD. Student's t-test, *, $P < 0.05$; **, $P < 0.01$.